Accepted Manuscript

Comparisons of three kinds of plane wave methods for the Helmholtz equation and time-harmonic Maxwell equations with complex wave numbers

Long Yuan, Qiya Hu

PII: S0377-0427(18)30295-4
DOI: https://doi.org/10.1016/j.cam.2018.05.024
Reference: CAM 11689

To appear in: *Journal of Computational and Applied Mathematics*

Received date : 1 June 2017
Revised date : 14 March 2018

Please cite this article as: L. Yuan, Q. Hu, Comparisons of three kinds of plane wave methods for the Helmholtz equation and time-harmonic Maxwell equations with complex wave numbers, *Journal of Computational and Applied Mathematics* (2018), https://doi.org/10.1016/j.cam.2018.05.024

COMPARISONS OF THREE KINDS OF PLANE WAVE METHODS FOR THE HELMHOLTZ EQUATION AND TIME-HARMONIC MAXWELL EQUATIONS WITH COMPLEX WAVE NUMBERS *

LONG YUAN † AND QIYA HU ‡

Abstract. In this paper we are concerned with some plane wave discretization methods of the Helmholtz equation and time-harmonic Maxwell equations with complex wave numbers. We design two new variants of the variational theory of complex rays and the ultra weak variational formulation for the discretization of these types of equations, respectively. The well posedness of the approximate solutions generated by the two methods is derived. Moreover, based on the PWLS-LSFE method introduced in [16], we extend these two methods (VTCR method and UWVF method) combined with local spectral element to discretize nonhomogeneous Helmholtz equation and Maxwell's equatons. The numerical results show that the resulting approximate solution generated by the UWVF method is clearly more accurate than that generated by the VTCR method.

Key words. Helmholtz equation, time-harmonic Maxwell's equations, well posedness, electromagnetic wave, plane wave basis, error estimates

AMS subject classifications. 65N30, 65N55.

1. Introduction.

The plane wave method, which fall into the class of Trefftz methods [26], was first introduced to solve the Helmholtz equation. Examples of this approach include the Variational Theory of Complex Rays (VTCR) introduced in [22, 23], the Ultra Weak Variational Formulation (UWVF) (see [4, 5, 28]), the plane wave Lagrangian multiplier (PWLM) method [7, 25], the plane wave discontinuous Galerkin methods (PWDG) (see [9, 12, 31]) and the weighted plane wave least-squares (PWLS) method (see [14, 21, 29, 30, 27]). The plane wave discretization method have been extended to discretization of time-harmonic Maxwell equations recently (see [13, 15, 17]). The plane wave methods have an important advantage over the other methods for discretization of the Helmholtz equation and time-harmonic Maxwell equations: the resulting approximate solutions have higher accuracies, owing mainly to the choice of the basis functions satisfying the governing differential equation without boundary conditions.

Recently, the UWVF method was extended to solve Maxwell's equations in [17, 18]. The studies [17, 18] were devoted to computing the electric and magnetic fields in a non-absorbing medium or within the PML. It was pointed out in [17] (p.733) that *the permittivity of the material in the computational domain for Maxwell's equations is, in general, complex valued* (i.e., the material is an absorbing medium). Moreover, the study [17] provides a procedure based on the UWVF method to compute the fields in absorbing media. This procedure shows that a postprocessing step is needed in the case of an absorbing medium. In the recently published work [15], the PWLS method was extended to discretize the time-harmonic Maxwell equations in absorbing media, and the numerical results indicate that the approximate solution generated by the method is much more accurate than that generated by the UWVF method. Moreover, the VTCR method and PWDG method have not been extended to discretize the Helmholtz equation and time-harmonic Maxwell equations with complex

*The first author was supported by China NSF under the grant 11501529, Qinddao applied basic research project under grant 17-1-1-9-jch and Scientific Research Foundation of Shandong University of Science and Technology for Recruited Talents. The second author was supported by the Natural Science Foundation of China G11571352.

† College of Mathematics and Systems Science, Shandong University of Science and Technology, 579 QIAN WAN GANG ROAD, Qingdao 266590, China (yuanlong@lsec.cc.ac.cn).

‡1. LSEC, Institute of Computational Mathematics and Scientic/Engineering Computing, Academy of Mathematics and Systems Science, Chinese Academy of Sciences, Beijing 100190, China; 2. School of Mathematical Sciences, University of Chinese Academy of Sciences, Beijing 100049, China (hqy@lsec.cc.ac.cn).

wavenumbers.

In this paper, the new variants of the VTCR method and the UWVF method are proposed to discretize the Helmholtz equation and time-harmonic Maxwell equations with complex wavenumbers. The new UWVF method differs from the existing UWVF method (see [4, 17]) in the sense that the trial function space is different from the test function space. Moreover, we introduce a way following [16] to discretize nonhomogeneous Helmholtz equation and Maxwell's equatons by these methods combined with local spectral element. For convenience, we call these two methods as VTCR-LSFE and UWVF-LSFE methods, respectively. Rates of convergence for the UWVF-LSFE method are proved and verified numerically in one special case of real wavenumbers. Numerical experiments show that the new UWVF method is obviously superior to the new VTCR method, and the UWVF method is comparable to the PWLS method in the numerical accuracy.

The paper is organized as follows: In Section 2, we describe the proposed VTCR method for the Helmholtz equation and time-harmonic Maxwell's equations with complex wavenumbers. In Section 3, we describe the proposed UWVF method for the Helmholtz equation and time-harmonic Maxwell's equations with complex wavenumbers. In Section 4, we explain how to discretize the resulting variational problems. In Section 5, we introduce a way to discretize nonhomogeneous Helmholtz equation and Maxwell's equatons by these methods combined with local spectral element. Finally, in Section 6, we report some numerical results to confirm the effectiveness of several methods.

2. A new variant of the VTCR method for the equations with complex wavenumbers. In this section we introduce a new variational formulation for the Helmholtz equation with complex wave numbers.

The considered variational formulations are based on a triangulation of the solution domain. Let Ω be the underlying domain in $\mathbb{R}^n$ ($n = 2, 3$). For convenience, assume that Ω is a bounded polygon or polyhedron. Let Ω be decomposed into the union of some subdomains in the sense that

$$\overline{\Omega} = \bigcup_{k=1}^{N} \overline{\Omega}_k, \quad \Omega_l \bigcap \Omega_j = \emptyset \quad \text{for } l \neq j,$$

where each Ω_k is a polygon (for two-dimensional case) or polyhedron (for three-dimensional case). Let $\mathcal{T}_h$ denote the triangulation comprising the elements $\{\Omega_k\}$, where h is the meshwidth of the triangulation. As usual, we assume that $\mathcal{T}_h$ is quasi-uniform and regular. Define

$$\Gamma_{lj} = \partial\Omega_l \bigcap \partial\Omega_j \quad \text{for } l \neq j$$

and

$$\gamma_k = \overline{\Omega}_k \bigcap \partial\Omega \quad (k = 1, \ldots, N), \quad \gamma = \bigcup_{k=1}^{N} \gamma_k.$$

2.1. The case of Helmholtz equation. Consider the Helmholtz equation with the mixed boundary conditions.

$$\text{(2.1)} \qquad \left\{ \begin{array}{rcll} -\Delta u - \kappa^2 u & = & 0 & \text{in} \quad \Omega, \\ u & = & g_d & \text{on} \quad \gamma_d, \\ \frac{\partial u}{\partial \mathbf{n}} & = & g_n & \text{on} \quad \gamma_n, \\ \frac{\partial u}{\partial \mathbf{n}} + i\kappa u & = & g_r & \text{on} \quad \gamma_r. \end{array} \right.$$

The outer normal derivative is referred to by $\partial_{\mathbf{n}}$ and the wavenumber by κ. In particular, if κ is complex valued, then the material is known as a lossy medium; otherwise the material is called a non-lossy medium (see [19]).

Each element Ω_k is subjected to excitations applied along $\partial\Omega_k = \gamma_d \bigcup \gamma_n \bigcup \gamma_r \bigcup \gamma_{kj}$ in the form of a Dirichlet condition over γ_d, a Neumann condition over γ_n, a Robin condition over γ_r. Moreover, $g_d \in L^2(\gamma_d), g_n \in L^2(\gamma_n), g_r \in L^2(\gamma_r)$.

Set $u|_{\Omega_k} = u_k$ $(k = 1, \cdots, N)$. Then the reference problem to be solved consists in finding the local acoustic pressures $u_k \in H^1(\Omega_k)$ such that

$$\begin{cases} -\Delta u_k - \kappa^2 u_k = 0 & \text{in} \quad \Omega_k, \\ u = g_d & \text{on} \quad \gamma_d \subset \partial\Omega_k, \\ \frac{\partial u}{\partial \mathbf{n}} = g_n & \text{on} \quad \gamma_n \subset \partial\Omega_k, \\ \frac{\partial u}{\partial \mathbf{n}} + i\kappa u = g_r & \text{on} \quad \gamma_r \subset \partial\Omega_k, \end{cases} \qquad (k = 1, 2, \ldots, N), \tag{2.2}$$

and

$$\begin{cases} u_k - u_j = 0 & \text{over} \quad \Gamma_{kj}, \\ \partial_{\mathbf{n}_k} u_k + \partial_{\mathbf{n}_j} u_j = 0 & \text{over} \quad \Gamma_{kj}. \end{cases} \qquad (k \neq j;\ k, j = 1, 2, \cdots, N). \tag{2.3}$$

The first equation of (2.2) is the homogeneous Helmholtz equation, The other equations of (2.2) and the equations (2.3) are related to the boundary condition of the problem and the continuity conditions at the interface between the subcavities Ω_k and Ω_j.

Let $V(\Omega_k)$ denote the space of the functions which verify Helmholtz's homogeneous equation (2.1) on the cavity Ω_k:

$$V(\Omega_k) = \{v_k \in H^1(\Omega_k);\ \Delta v_k + \kappa^2 v_k = 0\}. \tag{2.4}$$

Define

$$V(\mathcal{T}_h) = \prod_{k=1}^{N} V(\Omega_k). \tag{2.5}$$

Following the original VTCR method ([22, 23]), a new variant for the case of the complex wavenumbers can be expressed as follows: find $u \in V(\mathcal{T}_h)$ such that

(2.6)

$$\begin{aligned} Re\bigg\{ & \int_{\gamma_d} (u - g_d) \cdot \overline{i\partial_{\mathbf{n}} v} ds + \int_{\gamma_n} \overline{i(\partial_{\mathbf{n}} u - g_n)} \cdot v ds \\ & + \int_{\gamma_r} \frac{1}{2}\Big(\big((\partial_{\mathbf{n}} + i\kappa)u - g_r\big) \cdot \overline{\frac{-1}{\overline{\kappa}} \partial_{\mathbf{n}} v} + \overline{i\big((\partial_{\mathbf{n}} + i\kappa)u - g_r\big) \cdot v}\Big) ds \\ & + \sum_{j \neq k} \frac{1}{2} \int_{\Gamma_{kj}} \Big((u_k - u_j) \cdot \overline{i(\partial_{\mathbf{n}_k} v_k - \partial_{\mathbf{n}_j} v_j)} + \overline{i(\partial_{\mathbf{n}_k} u_k + \partial_{\mathbf{n}_j} u_j) \cdot (v_k + v_j)} \Big) ds \bigg\} = 0, \forall v \in V(\mathcal{T}_h), \end{aligned}$$

where $Re\{\diamond\}$ designate the real part of the complex quantity $\diamond$.

Theorem 2.1. *Let $u \in V(\mathcal{T}_h), Im(\kappa) < 0$. For $k = 1, \cdots, N$, assume that $u_k \in H^{1+\delta_k}(\Omega_k)$ with $\delta_k > \frac{1}{2}$ such that $\partial_{\mathbf{n}_k} u_k \in L^2(\partial\Omega_k)$. Then the reference problem (2.2) and (2.3) is equivalent to the new variational problem (2.6).*

Proof. It is clear that the solution of the problem (2.2) and (2.3) is also the solution of the variational problem (2.6). Therefore one needs only to verify the uniqueness of solution of the problem (2.6).

The verification is standard. Let us consider two solutions $u = (u_1, \cdots, u_N), u' = (u'_1, \cdots, u'_N)$ of the variational problem (2.6), and let $\tilde{u} = (\tilde{u}_1, \cdots, \tilde{u}_N)$ denote the difference between the two solutions. Because of (2.6), these two solutions must verify the following equation:

(2.7)
$$Re\Big\{ \int_{\gamma_d} \tilde{u} \cdot \overline{i\partial_{\mathbf{n}} v} ds + \int_{\gamma_n} \overline{i\partial_{\mathbf{n}} \tilde{u}} \cdot v ds + \int_{\gamma_r} \frac{1}{2}\Big((\partial_{\mathbf{n}} + i\kappa)\tilde{u} \cdot \overline{\frac{-1}{\overline{\kappa}} \partial_{\mathbf{n}} v} + \overline{i(\partial_{\mathbf{n}} + i\kappa)\tilde{u}} \cdot v \Big) ds$$
$$+ \sum_{j\neq k} \frac{1}{2} \int_{\Gamma_{kj}} \Big((\tilde{u}_k - \tilde{u}_j) \cdot \overline{i(\partial_{\mathbf{n}_k} v_k - \partial_{\mathbf{n}_j} v_j)} + \overline{i(\partial_{\mathbf{n}_k} \tilde{u}_k + \partial_{\mathbf{n}_j} \tilde{u}_j)} \cdot (v_k + v_j) \Big) ds \Big\} = 0, \forall v \in V(\mathcal{T}_h).$$

Taking $v = \tilde{u}$, (2.7) simplifies to

$$Re\Big\{ \sum_{k=1}^{N} \int_{\partial\Omega_k} \tilde{u}_k \cdot \overline{i\partial_{\mathbf{n}} \tilde{u}_k} ds + \int_{\gamma_r} \frac{1}{2}\Big(-\frac{1}{\kappa} \partial_{\mathbf{n}} \tilde{u} \cdot \overline{\partial_{\mathbf{n}} \tilde{u}} - \overline{\kappa \tilde{u}} \cdot \tilde{u} \Big) ds \Big\} = 0. \tag{2.8}$$

The Strokes formula applied to each subcavity Ω_k yields

$$Re\Big\{ \sum_{k=1}^{N} (-i) \int_{\Omega_k} \Big(\nabla \tilde{u}_k \cdot \overline{\nabla \tilde{u}_k} + \tilde{u}_k \cdot \overline{\triangle \tilde{u}_k} \Big) d\boldsymbol{x} + \int_{\gamma_r} \frac{1}{2}\Big(-\frac{1}{\kappa} \partial_{\mathbf{n}} \tilde{u} \cdot \overline{\partial_{\mathbf{n}} \tilde{u}} - \overline{\kappa \tilde{u}} \cdot \tilde{u} \Big) ds \Big\} = 0, \tag{2.9}$$

which, since $\tilde{u} \in V(\mathcal{T}_h)$, becomes

$$Re\Big\{ \sum_{k=1}^{N} (-i) \int_{\Omega_k} \Big(\nabla \tilde{u}_k \cdot \overline{\nabla \tilde{u}_k} - \overline{k}^2 \tilde{u}_k \cdot \overline{\tilde{u}_k} \Big) d\boldsymbol{x} + \int_{\gamma_r} \frac{1}{2}\Big(-\frac{1}{\kappa} \partial_{\mathbf{n}} \tilde{u} \cdot \overline{\partial_{\mathbf{n}} \tilde{u}} - \overline{\kappa \tilde{u}} \cdot \tilde{u} \Big) ds \Big\} = 0. \tag{2.10}$$

Set $\kappa = \kappa_1 + i\kappa_2$, then (2.10) simplifies trivially to

$$\sum_{k=1}^{N} \int_{\Omega_k} 2\kappa_1\kappa_2 \tilde{u}_k \cdot \overline{\tilde{u}_k} d\boldsymbol{x} - \frac{1}{2} \int_{\gamma_r} \Big(\kappa_1 \overline{\tilde{u}} \cdot \tilde{u} + \frac{\kappa_1}{\kappa_1^2 + \kappa_2^2} \partial_{\mathbf{n}} \tilde{u} \cdot \overline{\partial_{\mathbf{n}} \tilde{u}} \Big) ds = 0. \tag{2.11}$$

By the assumption $Im(\kappa) < 0$, we can deduce that $\tilde{u}_k = 0$ in Ω_k. Thus, by the assumption $u_k \in H^{1+\delta_k}(\Omega_k)$ with $\delta_k > \frac{1}{2}$, we obtain the function $\tilde{u}$ satisfies the interface continuity (2.3) and verifies the initial Helmholtz reference problem (2.2) (note that $\tilde{u} \in V(\mathcal{T}_h)$) with the homogeneous boundary condition. Therefore $\tilde{u}$ vanishes on Ω, which proves the uniqueness of solution (2.6). □

2.2. The case of Maxwell's equation. In this section we recall the first-order system of Maxwell equations and derive the corresponding Variational Theory of Complex Rays based on triangulation.

Suppose Ω is a bounded polyhedral domain in $\mathbb{R}^3$. We want to compute a numerical approximation of the electromagnetic field $(\mathbf{E}, \mathbf{H})$ solution of the harmonic three-dimensional (3D) homogeneous Maxwell equations written as a first-order system of equations (refer to [17]):

$$\begin{cases} \nabla \times \mathbf{E} - i\omega\mu\mathbf{H} = 0 \\ \nabla \times \mathbf{H} + i\omega\varepsilon\mathbf{E} = 0 \end{cases} \quad in \quad \Omega \tag{2.12}$$

with the following mixed boundary conditions

$$\begin{cases} -\mathbf{E} \times \mathbf{n} = \mathbf{g}_d & \text{on} \quad \gamma_d, \\ \mathbf{H} \times \mathbf{n} \times \mathbf{n} = \mathbf{g}_n & \text{on} \quad \gamma_n, \\ -\mathbf{E} \times \mathbf{n} + \sigma(\mathbf{H} \times \mathbf{n}) \times \mathbf{n} = \mathbf{g}_r & \text{on} \quad \gamma_r. \end{cases} \tag{2.13}$$

Here, $\omega > 0$ is the temporal frequency of the field, and $\mathbf{g} \in L^2_{\mathbf{T}}(\partial\Omega)$. The material coefficients $\mu > 0, \varepsilon$ and $\sigma = \sqrt{\frac{\mu}{|\varepsilon|}}$ are understood as usual (refer to [17]). In particular, if ε is complex valued, then the material is known as an absorbing medium; otherwise the material is called a non-absorbing medium (see [17]).

For each element Ω_k, let $\mathbf{E}|_{\Omega_k} = \mathbf{E}_k, \mathbf{H}|_{\Omega_k} = \mathbf{H}_k$ $(k = 1, \ldots, N)$. As usual, we assume that ω, μ and ε are constants on each element. Then the reference problem (2.12) to be solved consists of finding the local electric field $(\mathbf{E}_k, \mathbf{H}_k)$ such that

$$\begin{cases} \nabla \times \mathbf{E}_k - i\omega\mu\mathbf{H}_k = 0 \\ \nabla \times \mathbf{H}_k + i\omega\varepsilon\mathbf{E}_k = 0 \end{cases} \quad in \quad \Omega_k, \tag{2.14}$$

namely,

$$\nabla \times (\nabla \times \mathbf{E}_k) - \kappa^2 \mathbf{E}_k = 0 \quad \text{in} \quad \Omega_k \tag{2.15}$$

with the complex wavenumber $\kappa = \omega\sqrt{\mu\varepsilon}$, and the interface conditions (note that $\mathbf{n}_l = -\mathbf{n}_j$)

$$\begin{cases} \mathbf{E}_l \times \mathbf{n}_l + \mathbf{E}_j \times \mathbf{n}_j = 0 \\ \mathbf{H}_l \times \mathbf{n}_l + \mathbf{H}_j \times \mathbf{n}_j = 0 \end{cases} \quad \text{on} \quad \Gamma_{lj} \quad (l < j;\ l, j = 1, 2, \ldots, N). \tag{2.16}$$

The boundary condition becomes

$$\begin{cases} -\mathbf{E}_k \times \mathbf{n}_k = \mathbf{g}_d & \text{on} \quad \gamma_{d,k} = \gamma_d \cap \partial\Omega_k, \\ \mathbf{H}_k \times \mathbf{n}_k \times \mathbf{n}_k = \mathbf{g}_n & \text{on} \quad \gamma_{n,k} = \gamma_n \cap \partial\Omega_k, \\ -\mathbf{E}_k \times \mathbf{n}_k + \sigma(\mathbf{H}_k \times \mathbf{n}_k) \times \mathbf{n}_k = \mathbf{g}_r & \text{on} \quad \gamma_{r,k} = \gamma_r \cap \partial\Omega_k. \end{cases} \tag{2.17}$$

Define the trial space

$$\mathbf{U}(\mathcal{T}_h) = \left\{ \mathbf{u} = \begin{pmatrix} \mathbf{E} \\ \mathbf{H} \end{pmatrix}, \mathbf{u}|_{\Omega_k} = \mathbf{u}_k \middle| \begin{cases} \nabla \times \mathbf{E}_k - i\omega\mu\mathbf{H}_k = 0 \\ \nabla \times \mathbf{H} + i\omega\varepsilon\mathbf{E} = 0 \end{cases} \quad \text{in} \quad \Omega_k \right\}. \tag{2.18}$$

Based on the above equivalence and the procedure of VTCR method for the Helmholtz e-quation with complex wavenumbers, we define the new variational formulation: find $(\mathbf{E}, \mathbf{H}) \in \mathbf{U}(\mathcal{T}_h)$, such that

(2.19)

$$\begin{aligned} Re\Bigg\{ &\int_{\gamma_d} (-\mathbf{E} \times \mathbf{n} - \mathbf{g}_d) \cdot \overline{i\boldsymbol{\xi} \times \mathbf{n} \times \mathbf{n}} ds + \int_{\gamma_n} \overline{i(\mathbf{H} \times \mathbf{n} \times \mathbf{n} - \mathbf{g}_n)} \cdot (-\boldsymbol{\psi} \times \mathbf{n}) ds \\ &+ \int_{\gamma_r} \frac{1}{2}\Big(\big(-\mathbf{E} \times \mathbf{n} + \sigma(\mathbf{H} \times \mathbf{n}) \times \mathbf{n} - \mathbf{g}_r\big) \cdot \overline{i\boldsymbol{\xi} \times \mathbf{n} \times \mathbf{n}} \\ &+ \overline{i\big(-\mathbf{E} \times \mathbf{n} + \sigma(\mathbf{H} \times \mathbf{n}) \times \mathbf{n} - \mathbf{g}_r\big)} \cdot \frac{1}{\sigma}(-\boldsymbol{\psi} \times \mathbf{n})\Big) ds \\ &+ \sum_{j \neq k} \frac{1}{2} \int_{\Gamma_{kj}} \Big((-\mathbf{E}_k \times \mathbf{n}_k - \mathbf{E}_j \times \mathbf{n}_j) \cdot \overline{i\big((\boldsymbol{\xi}_k \times \mathbf{n}_k) \times \mathbf{n}_k + (\boldsymbol{\xi}_j \times \mathbf{n}_j) \times \mathbf{n}_j\big)} \\ &+ \overline{i\big((\boldsymbol{H}_k \times \mathbf{n}_k) \times \mathbf{n}_k - (\boldsymbol{H}_j \times \mathbf{n}_j) \times \mathbf{n}_j\big)} \cdot (-\boldsymbol{\psi}_k \times \mathbf{n}_k + \boldsymbol{\psi}_j \times \mathbf{n}_j) \Big) ds \Bigg\} = 0, \forall (\boldsymbol{\psi}, \boldsymbol{\xi}) \in \mathbf{U}(\mathcal{T}_h). \end{aligned}$$

Theorem 2.2. *Let $(\mathbf{E}, \mathbf{H}) \in \mathbf{U}(\mathcal{T}_h), Re(\varepsilon) < 0$. For $k = 1, \cdots, N$, assume that $\mathbf{E}_k \in H^{1+\delta_k}(\Omega_k)$ with $\delta_k > \frac{1}{2}$ such that $\frac{1}{i\omega\mu}(\nabla \times \mathbf{E}_k) \times \mathbf{n}_k \times \mathbf{n}_k = \mathbf{H}_k \times \mathbf{n}_k \times \mathbf{n}_k \in L^2(\partial\Omega_k)$. Then the reference problem (2.14)-(2.17) is equivalent to the new variational problem (2.19).*

Proof. It is clear that the solution of the problem (2.14)-(2.17) is also the solution of the variational problem (2.19). Therefore one needs only to verify the uniqueness of solution of the problem (2.19).

Let us consider the following two solutions of the variational problem

$$\begin{pmatrix} \mathbf{E} = (\mathbf{E}_1, \ldots, \mathbf{E}_N) \\ \mathbf{H} = (\mathbf{H}_1, \ldots, \mathbf{H}_N) \end{pmatrix} \quad \text{and} \quad \begin{pmatrix} \mathbf{E}' = (\mathbf{E}'_1, \ldots, \mathbf{E}'_N) \\ \mathbf{H}' = (\mathbf{H}'_1, \ldots, \mathbf{H}'_N) \end{pmatrix}, \tag{2.20}$$

and let

$$\begin{pmatrix} \tilde{\mathbf{E}} = (\tilde{\mathbf{E}}_1, \ldots, \tilde{\mathbf{E}}_N) \\ \tilde{\mathbf{H}} = (\tilde{\mathbf{H}}_1, \ldots, \tilde{\mathbf{H}}_N) \end{pmatrix} \tag{2.21}$$

denote the difference between the two solutions. It follows by (2.19) that the difference satisfies

(2.22)

$$\begin{aligned} Re\Big\{ & \int_{\gamma_d} (-\tilde{\mathbf{E}} \times \mathbf{n}) \cdot \overline{i\boldsymbol{\xi} \times \mathbf{n} \times \mathbf{n}} ds + \int_{\gamma_n} \overline{i(\tilde{\mathbf{H}} \times \mathbf{n} \times \mathbf{n})} \cdot (-\psi \times \mathbf{n}) ds \\ & + \int_{\gamma_r} \frac{1}{2}\Big(\Big(-\tilde{\mathbf{E}} \times \mathbf{n} + \sigma(\tilde{\mathbf{H}} \times \mathbf{n}) \times \mathbf{n}\Big) \cdot \overline{i\boldsymbol{\xi} \times \mathbf{n} \times \mathbf{n}} \\ & + \overline{i\Big(-\tilde{\mathbf{E}} \times \mathbf{n} + \sigma(\tilde{\mathbf{H}} \times \mathbf{n}) \times \mathbf{n}\Big)} \cdot \frac{1}{\sigma}(-\psi \times \mathbf{n})\Big) ds \\ & + \sum_{j \neq k} \frac{1}{2} \int_{\Gamma_{kj}} \Big((-\tilde{\mathbf{E}}_k \times \mathbf{n}_k - \tilde{\mathbf{E}}_j \times \mathbf{n}_j) \cdot \overline{i\Big((\boldsymbol{\xi}_k \times \mathbf{n}_k) \times \mathbf{n}_k + (\boldsymbol{\xi}_j \times \mathbf{n}_j) \times \mathbf{n}_j\Big)} \\ & + \overline{i\Big((\tilde{\mathbf{H}}_k \times \mathbf{n}_k) \times \mathbf{n}_k - (\tilde{\mathbf{H}}_j \times \mathbf{n}_j) \times \mathbf{n}_j\Big)} \cdot (-\psi_k \times \mathbf{n}_k + \psi_j \times \mathbf{n}_j)\Big) ds \Big\} = 0, \forall (\psi, \boldsymbol{\xi}) \in \mathbf{U}(\mathcal{T}_h). \end{aligned}$$

Taking $\begin{pmatrix} \psi \\ \boldsymbol{\xi} \end{pmatrix} = \begin{pmatrix} \tilde{\mathbf{E}} \\ \tilde{\mathbf{H}} \end{pmatrix}$, (2.22) becomes

$$\begin{aligned} Re\Big\{ & \int_{\gamma_d} (-\tilde{\mathbf{E}} \times \mathbf{n}) \cdot \overline{i\tilde{\mathbf{H}} \times \mathbf{n} \times \mathbf{n}} ds + \int_{\gamma_n} \overline{i(\tilde{\mathbf{H}} \times \mathbf{n} \times \mathbf{n})} \cdot (-\tilde{\mathbf{E}} \times \mathbf{n}) ds \\ & + \int_{\gamma_r} \frac{1}{2}\Big(\Big(-\tilde{\mathbf{E}} \times \mathbf{n} + \sigma(\tilde{\mathbf{H}} \times \mathbf{n}) \times \mathbf{n}\Big) \cdot \overline{i\tilde{\mathbf{H}} \times \mathbf{n} \times \mathbf{n}} \\ & + \overline{i\Big(-\tilde{\mathbf{E}} \times \mathbf{n} + \sigma(\tilde{\mathbf{H}} \times \mathbf{n}) \times \mathbf{n}\Big)} \cdot \frac{1}{\sigma}(-\tilde{\mathbf{E}} \times \mathbf{n})\Big) ds \\ & + \sum_{j \neq k} \frac{1}{2} \int_{\Gamma_{kj}} \Big((-\tilde{\mathbf{E}}_k \times \mathbf{n}_k - \tilde{\mathbf{E}}_j \times \mathbf{n}_j) \cdot \overline{i\Big((\tilde{\mathbf{H}}_k \times \mathbf{n}_k) \times \mathbf{n}_k + (\tilde{\mathbf{H}}_j \times \mathbf{n}_j) \times \mathbf{n}_j\Big)} \\ & + \overline{i\Big((\tilde{\mathbf{H}}_k \times \mathbf{n}_k) \times \mathbf{n}_k - (\tilde{\mathbf{H}}_j \times \mathbf{n}_j) \times \mathbf{n}_j\Big)} \cdot (-\tilde{\mathbf{E}}_k \times \mathbf{n}_k + \tilde{\mathbf{E}}_j \times \mathbf{n}_j)\Big) ds \Big\} = 0. \end{aligned} \tag{2.23}$$

Then, by the simple calculation, we can deduce that

$$\begin{aligned} Re\Big\{ & \sum_{k=1}^{N} \int_{\partial\Omega_k} (-\tilde{\mathbf{E}} \times \mathbf{n}) \cdot \overline{i\tilde{\mathbf{H}} \times \mathbf{n} \times \mathbf{n}}\, ds \\ & + \frac{-i}{2} \int_{\gamma_r} (\sigma|\tilde{\mathbf{H}} \times \mathbf{n} \times \mathbf{n}|^2 + \frac{1}{\sigma}|-\tilde{\mathbf{E}} \times \mathbf{n}|^2)\, ds \Big\} = 0. \end{aligned} \tag{2.24}$$

This, together with (2.12) and simple calculation, leads to

$$
\begin{aligned}
Re\Big\{ \sum_{k=1}^{N}(-i)\int_{\partial\Omega_k} \overline{\mathbf{n}\times(\frac{1}{i\omega\mu}\nabla\times\tilde{\mathbf{E}})}\cdot\tilde{\mathbf{E}}\,ds \\
+\frac{-i}{2}\int_{\gamma_r}(\sigma|\tilde{\mathbf{H}}\times\mathbf{n}\times\mathbf{n}|^2+\frac{1}{\sigma}|-\tilde{\mathbf{E}}\times\mathbf{n}|^2)\,ds\Big\}=0.
\end{aligned}
\tag{2.25}
$$

Integrating by parts equation (2.25), we have

$$
\begin{aligned}
Re\Big\{ \sum_{k=1}^{N}(-i)\int_{\Omega_k}\Big(\overline{\nabla\times(\frac{1}{i\omega\mu}\nabla\times\tilde{\mathbf{E}})}\cdot\tilde{\mathbf{E}}-\overline{(\frac{1}{i\omega\mu}\nabla\times\tilde{\mathbf{E}})}\cdot\nabla\times\tilde{\mathbf{E}}\Big)\,d\boldsymbol{x} \\
+\frac{-i}{2}\int_{\gamma_r}(\sigma|\tilde{\mathbf{H}}\times\mathbf{n}\times\mathbf{n}|^2+\frac{1}{\sigma}|-\tilde{\mathbf{E}}\times\mathbf{n}|^2)\,ds\Big\}=0.
\end{aligned}
\tag{2.26}
$$

Using (2.12) again, we further get

$$
\begin{aligned}
Re\Big\{ \sum_{k=1}^{N}(-i)\int_{\Omega_k}\Big(\overline{-i\omega\varepsilon\tilde{\mathbf{E}}}\cdot\tilde{\mathbf{E}}-\overline{(\frac{1}{i\omega\mu}\nabla\times\tilde{\mathbf{E}})}\cdot\nabla\times\tilde{\mathbf{E}}\Big)\,d\boldsymbol{x} \\
+\frac{-i}{2}\int_{\gamma_r}(\sigma|\tilde{\mathbf{H}}\times\mathbf{n}\times\mathbf{n}|^2+\frac{1}{\sigma}|-\tilde{\mathbf{E}}\times\mathbf{n}|^2)\,ds\Big\}=0.
\end{aligned}
\tag{2.27}
$$

By the simple calculation, we have

$$
\begin{aligned}
Re\Big\{ \sum_{k=1}^{N}\int_{\Omega_k}\Big(\omega\overline{\varepsilon}|\tilde{\mathbf{E}}|^2-\frac{1}{\omega\mu}|\nabla\times\tilde{\mathbf{E}}|^2\Big)\,d\boldsymbol{x} \\
+\frac{-i}{2}\int_{\gamma_r}(\sigma|\tilde{\mathbf{H}}\times\mathbf{n}\times\mathbf{n}|^2+\frac{1}{\sigma}|-\tilde{\mathbf{E}}\times\mathbf{n}|^2)\,ds\Big\}=0.
\end{aligned}
\tag{2.28}
$$

Set $\varepsilon=\varepsilon_1+i\varepsilon_2$, then (2.28) simplifies trivially to

$$
\sum_{k=1}^{N}\int_{\Omega_k}\Big(\omega\varepsilon_1|\tilde{\mathbf{E}}|^2-\frac{1}{\omega\mu}|\nabla\times\tilde{\mathbf{E}}|^2\Big)\,d\boldsymbol{x}=0.
\tag{2.29}
$$

By the assumption $Re(\varepsilon)<0$, we can deduce that $\begin{pmatrix}\tilde{\mathbf{E}}\\ \tilde{\mathbf{H}}\end{pmatrix}=\begin{pmatrix}\mathbf{0}\\ \mathbf{0}\end{pmatrix}$ in Ω_k. Thus, by the assumption $\mathbf{E}_k\in H^{1+\delta_k}(\Omega_k)$ with $\delta_k>\frac{1}{2}$, we obtain the function $\begin{pmatrix}\tilde{\mathbf{E}}\\ \tilde{\mathbf{H}}\end{pmatrix}$ satisfies the interface continuity (2.16) and verifies the initial Maxwell reference problem (2.14) with the homogeneous boundary condition (2.17). Therefore $\begin{pmatrix}\tilde{\mathbf{E}}\\ \tilde{\mathbf{H}}\end{pmatrix}$ vanishes on Ω, which proves the uniqueness of solution (2.19). □

Remark 2.1. *We denote the inner part of* $Re\{\}$ *in (2.19) by the symbol* $\Upsilon(\mathbf{E},\mathbf{H},\boldsymbol{\psi},\boldsymbol{\xi})$*, then it can be verified that* $\forall(\boldsymbol{\psi},\boldsymbol{\xi})\in\mathbf{U}(\mathcal{T}_h)$*,*

$$
Re\{\Upsilon(\mathbf{E},\mathbf{H},\boldsymbol{\psi},\boldsymbol{\xi})\}=0 \quad \textit{is equivalent to that} \quad Im\{\Upsilon(\mathbf{E},\mathbf{H},\boldsymbol{\psi},\boldsymbol{\xi})\}=0.
\tag{2.30}
$$

By the (2.28), we can deduce that when $Im(\varepsilon)>0$*, the Theorem 2.2 also holds.*

Remark 2.2. *Note that for the case of real wavenumbers, the involved integrals on the Robin-type boundary condition of the original method and the new method are the same.*

Thus, there is no change between the two methods when dealing with real wavenumbers. For the case of complex wavenumbers, there are some differences between the two methods on the following.

(i) The original VTCR method can only be used to solve the Helmholtz equation with real wavenumbers. However, the permittivity of the material in the computational domain for the Helmholtz and Maxwell equations is, in general, complex valued. By selecting the involved integral defined on the Robin-type boundary condition, the new method is proposed to solve the Helmholtz equation and Maxwell equations with complex wavenumbers.

(ii) The variational formulation of the new method is unified when dealing with real wavenumbers and complex wavenumbers.

3. A new variant of the UWVF method for the equations with complex wavenumbers. In this section we introduce a new variant of the UWVF method for the Helmholtz equation and Maxwell equations with complex wave numbers.

3.1. The case of Helmholtz equation. The purpose of this section is to recall the basic principles of the UWVF modeling methodology for the resolution of the Helmholtz equation. At first, the original UWVF method is recalled. Then the new variant is presented in details.

3.1.1. The original UWVF method. The following Helmholtz equation is considered.

$$\left\{\begin{array}{lcll} -\Delta u-\kappa^2 u & = & 0 & \text{in} \quad \Omega, \\ \frac{\partial u}{\partial \mathbf{n}}+i\kappa u & = & t(-\frac{\partial u}{\partial \mathbf{n}}+i\kappa u)+g & \text{on} \quad \gamma, \\ |t|<1, & & t\in C. & \end{array}\right. \tag{3.1}$$

Similar to the VTCR method, the reference problem (3.1) is equivalent to the problem

$$\left\{\begin{array}{ll} -\Delta u_k-\kappa^2 u_k=0 & \text{in} \quad \Omega_k, \\ \frac{\partial u}{\partial \mathbf{n}}+i\kappa u=t(-\frac{\partial u}{\partial \mathbf{n}}+i\kappa u)+g & \text{on} \quad \gamma\bigcap\partial\Omega_k, \end{array}\right. \qquad (k=1,2,\ldots,N), \tag{3.2}$$

and the interface conditions (2.3).

Let us recall the original UWVF method (see, for example, [4]). Let V denote the space of the functions of the UWVF formulation as

$$V=\prod_{k=1}^{N} L^2(\partial\Omega_k). \tag{3.3}$$

The value of the unknown x of the UWVF formulation will be defined from u solution of (3.1) as being

$$x|_{\partial\Omega_k}=(-\partial_{\mathbf{n}_k}+i\kappa)u_k, \tag{3.4}$$

assuming the regularity hypothesis $x\in V$. Then the variational problem for the case of real wavenumbers can be expressed as follows: find $x\in V$ defined by $x|_{\partial\Omega_k}=x_k$ with (3.4) such that

$$\begin{aligned} &\Big(\sum_k \int_{\partial\Omega_k} x_k\overline{(-\partial_{\mathbf{n}_k}+i\kappa)e_k}\,ds\Big) \\ &-\Big(\sum_{k\neq j}\int_{\Gamma_{kj}} x_j\overline{(\partial_{\mathbf{n}_k}+i\kappa)e_k}\,ds+\sum_k\int_{\gamma_k} tx_k\overline{(\partial_{\mathbf{n}_k}+i\kappa)e_k}\,ds\Big) \\ &=\sum_k\int_{\gamma_k} g\,\overline{(\partial_{\mathbf{n}_k}+i\kappa)e_k}\,ds \end{aligned} \tag{3.5}$$

for any

$$e \in H, e|_{\Omega_k} = e_k, H = \prod_{k=1}^{N} H_k \tag{3.6}$$

with

$$H_k = \left\{ v_k \in H^1(\Omega_k) \text{ satisfying } \left\{ \begin{array}{l} (-\Delta - \kappa^2)v_k = 0 \quad \text{in} \quad \Omega_k \\ (-\partial_{\mathbf{n}_k} + i\kappa)v_k \in L^2(\partial\Omega_k) \end{array} \right. \right\}. \tag{3.7}$$

Conversely, if x is solution of (3.5), then the function u defined by

$$\left\{ \begin{array}{l} u|_{\Omega_k} = u_k, \\ (-\Delta - \kappa^2)u_k = 0 \\ (-\partial_{\mathbf{n}_k} + i\kappa)u_k = x_k, \end{array} \right. \tag{3.8}$$

where $u_k \in H^1(\Omega_k)$ is the unique solution of (3.1).

Note that the original UWVF method was obtained only for the case of real wavenumbers, so how to generalize the UWVF method to the equations with complex wavenumbers is an interesting problem. In the next subsection, we propose a new variant of the UWVF method.

3.1.2. A new variant of the UWVF method. Our main idea is to use the different trial space and test space, in which the functions satisfy the original equation and adjoint equation, respectively. Thus, the new variant of the UWVF method is essentially a discontinuous Petrov-Galerkin method.

Let $W(\mathcal{T}_h)$ denote the test space, satisfying $W(\mathcal{T}_h) = \prod_{k=1}^{N} W_k(\Omega_k)$ with

$$W_k(\Omega_k) = \left\{ e_k \in H^1(\Omega_k) \text{ satisfying } \left\{ \begin{array}{l} (-\Delta - \overline{\kappa}^2)e_k = 0 \quad \text{in} \quad \Omega_k \\ (-\partial_{\mathbf{n}_k} + i\,\overline{\kappa}\,)e_k \in L^2(\partial\Omega_k) \end{array} \right. \right\}. \tag{3.9}$$

Then we get the following theorem.

Theorem 3.1. *Let $u \in V(\mathcal{T}_h)$ (see (2.5)) satisfy the regularity assumption $\partial_{\mathbf{n}_k} u \in L^2(\partial\Omega_k)$, $k = 1, \cdots, N$ and be a solution of the original equation (3.1). Then the reference problem (3.1) is equivalent to the following new variational problem (3.10).*

$$\begin{aligned} &\Big(\sum_k \int_{\partial\Omega_k} (-\partial_{\mathbf{n}_k} + i\kappa)u_k \overline{(-\partial_{\mathbf{n}_k} + i\,\overline{\kappa}\,)e_k}\, ds \Big) \\ &- \Big(\sum_{k \neq j} \int_{\Gamma_{kj}} (-\partial_{\mathbf{n}_j} + i\kappa)u_j \overline{(\partial_{\mathbf{n}_k} + i\,\overline{\kappa}\,)e_k}\, ds + \sum_k \int_{\gamma_k} t(-\partial_{\mathbf{n}_k} + i\kappa)u_k \overline{(\partial_{\mathbf{n}_k} + i\,\overline{\kappa}\,)e_k}\, ds \Big) \\ &= \sum_k \int_{\gamma_k} g\, \overline{(\partial_{\mathbf{n}_k} + i\,\overline{\kappa}\,)e_k}\, ds, \quad \forall e \in W(\mathcal{T}_h). \end{aligned} \tag{3.10}$$

Proof. Since $u \in H^1(\Omega)$ and $\partial_{\mathbf{n}_k} u \in L^2(\partial\Omega_k)$, we get

$$\begin{aligned} &\int_{\partial\Omega_k} (-\partial_{\mathbf{n}_k} + i\kappa)u \overline{(-\partial_{\mathbf{n}_k} + i\,\overline{\kappa}\,)e_k}\, ds \\ &= \int_{\partial\Omega_k} (\partial_{\mathbf{n}_k} + i\kappa)u \overline{(\partial_{\mathbf{n}_k} + i\,\overline{\kappa}\,)e_k}\, ds + 2i\kappa \int_{\partial\Omega_k} (\partial_{\mathbf{n}_k} u\, \overline{e_k} - u\, \overline{\partial_{\mathbf{n}_k} e_k}\,)\, ds. \end{aligned} \tag{3.11}$$

Using (3.1) and (3.9), and by integrations by parts, we can deduce that

$$\left\{\begin{array}{l}\int_{\Omega_k} \nabla u\, \overline{\nabla e_k} - \kappa^2 u\, \overline{e_k} = \int_{\partial\Omega_k} u\, \overline{\partial_{\mathbf{n}_k} e_k},\\ \int_{\Omega_k} \nabla u\, \overline{\nabla e_k} - \kappa^2 u\, \overline{e_k} = \int_{\partial\Omega_k} \partial_{\mathbf{n}_k} u\, \overline{e_k}.\end{array}\right. \tag{3.12}$$

From (3.11) and (3.12), we have

$$\begin{aligned}&\int_{\partial\Omega_k} (-\partial_{\mathbf{n}_k} + i\kappa)u\, \overline{(-\partial_{\mathbf{n}_k} + i\,\overline{\kappa}\,)e_k}\, ds\\ &- \int_{\partial\Omega_k} (\partial_{\mathbf{n}_k} + i\kappa)u\, \overline{(\partial_{\mathbf{n}_k} + i\,\overline{\kappa}\,)e_k}\, ds \;=\; 0.\end{aligned} \tag{3.13}$$

This, together with the continuity of u on Γ_{kj} and the boundary condition

$$\left\{\begin{array}{l}(\partial_{\mathbf{n}_k} + i\kappa)u|_{\Gamma_{kj}} = (-\partial_{\mathbf{n}_j} + i\kappa)u|_{\Gamma_{jk}}\\ (\partial_{\mathbf{n}_k} + i\kappa)u|_{\gamma_k} = t(-\partial_{\mathbf{n}_k} + i\kappa)u|_{\gamma_k} + g,\end{array}\right. \tag{3.14}$$

and summing for all elements k, leads to the desired equation (3.10).

Conversely, let u be solution of (3.10). By assumptions on u and e, we obtain (3.13). Summing on all the elements, we have

$$\begin{aligned}&\sum_k \int_{\partial\Omega_k} (-\partial_{\mathbf{n}_k} + i\kappa)u\, \overline{(-\partial_{\mathbf{n}_k} + i\,\overline{\kappa}\,)e_k}\, ds\\ &- \sum_k \int_{\partial\Omega_k} (\partial_{\mathbf{n}_k} + i\kappa)u\, \overline{(\partial_{\mathbf{n}_k} + i\,\overline{\kappa}\,)e_k}\, ds \;=\; 0.\end{aligned} \tag{3.15}$$

Since u satisfies (3.10) and combining with (3.15), we have

$$\left\{\begin{array}{l}\forall e \in W(\mathcal{T}_h),\\ \sum\limits_{k,j} \int_{\Gamma_{kj}} (\partial_{\mathbf{n}_k} + i\kappa)u\, \overline{(\partial_{\mathbf{n}_k} + i\,\overline{\kappa}\,)e_k}\, ds + \sum\limits_k \int_{\gamma_k} (\partial_{\mathbf{n}_k} + i\kappa)u\, \overline{(\partial_{\mathbf{n}_k} + i\,\overline{\kappa}\,)e_k}\, ds\\ = \sum\limits_{k,j} \int_{\Gamma_{kj}} x_j\, \overline{(\partial_{\mathbf{n}_k} + i\,\overline{\kappa}\,)e_k}\, ds + \sum\limits_k \int_{\gamma_k} (tx_k + g)\, \overline{(\partial_{\mathbf{n}_k} + i\,\overline{\kappa}\,)e_k}\, ds.\end{array}\right. \tag{3.16}$$

This yields (3.14). It is clear that a function whose restrictions are $H^1(\Omega_k)$ solutions of the elemental homogeneous Helmholtz equation and that satisfies the continuity conditions and outer boundary conditions (3.14) is the unique solution of the Helmholtz problem (3.1). □

3.2. The case of Maxwell's equations. In this section we generalize the UWVF method to the following Maxwell equations.

$$\left\{\begin{array}{lr}\nabla \times \mathbf{E} - i\omega\mu\mathbf{H} = 0 & in \quad \Omega,\\ \nabla \times \mathbf{H} + i\omega\varepsilon\mathbf{E} = 0 & in \quad \Omega,\\ -\mathbf{E} \times \mathbf{n} - \sigma(\mathbf{H} \times \mathbf{n}) \times \mathbf{n} = Q(-\mathbf{E} \times \mathbf{n} + \sigma(\mathbf{H} \times \mathbf{n}) \times \mathbf{n}) + \mathbf{g} & on \quad \gamma = \partial\Omega.\end{array}\right. \tag{3.17}$$

Our main idea is also to construct the correct spaces for the different trial space and test space. The trial space $\mathbf{U}(\mathcal{T}_h)$ is defined by (2.18).

Let $\boldsymbol{\xi}$ and $\boldsymbol{\psi}$ denote piecewise smooth test vector functions in the mesh. Using the integration by parts identity we obtain

$$\left\{\begin{array}{l}\int_{\Omega_k} (-i\omega\varepsilon\mathbf{E} \cdot \overline{\boldsymbol{\xi}_k} - \mathbf{H} \cdot \nabla \times \overline{\boldsymbol{\xi}_k})\, d\boldsymbol{x} = \int_{\partial\Omega_k} \mathbf{n}_k \times \mathbf{H} \cdot \overline{\boldsymbol{\xi}_k}\, ds,\\ \int_{\Omega_k} (-i\omega\mu\mathbf{H} \cdot \overline{\boldsymbol{\psi}_k} + \mathbf{E} \cdot \nabla \times \overline{\boldsymbol{\psi}_k})\, d\boldsymbol{x} = -\int_{\partial\Omega_k} \mathbf{n}_k \times \mathbf{E} \cdot \overline{\boldsymbol{\psi}_k}\, ds.\end{array}\right. \tag{3.18}$$

Adding the two equations we get

$$(3.19)\quad \int_{\Omega_k} (\mathbf{E}\cdot\overline{i\omega\bar{\varepsilon}\boldsymbol{\xi}_k + \nabla\times\boldsymbol{\psi}_k} + \mathbf{H}\cdot\overline{i\omega\mu\boldsymbol{\psi}_k - \nabla\times\boldsymbol{\xi}_k})\,d\boldsymbol{x} = \int_{\partial\Omega_k} (\mathbf{n}_k\times\mathbf{H}\cdot\overline{\boldsymbol{\xi}_k} - \mathbf{n}_k\times\mathbf{E}\cdot\overline{\boldsymbol{\psi}_k})\,ds.$$

We define the test space as follows.

$$(3.20)\qquad \mathbf{V}(\mathcal{T}_h) = \left\{\mathbf{v} = \begin{pmatrix}\boldsymbol{\xi}\\ \boldsymbol{\psi}\end{pmatrix}, \mathbf{v}|_{\Omega_k} = \mathbf{v}_k \middle| \begin{cases} i\omega\bar{\varepsilon}\boldsymbol{\xi}_k + \nabla\times\boldsymbol{\psi}_k = 0 \\ i\omega\mu\boldsymbol{\psi}_k - \nabla\times\boldsymbol{\xi}_k = 0 \end{cases} \text{in} \quad \Omega_k\right\}.$$

With the definition of the test space, (3.19) reduces to

$$(3.21)\qquad \int_{\partial\Omega_k} (\mathbf{n}_k\times\mathbf{H}\cdot\overline{\boldsymbol{\xi}_k} - \mathbf{n}_k\times\mathbf{E}\cdot\overline{\boldsymbol{\psi}_k})\,ds = 0.$$

We further get

$$(3.22)\qquad \int_{\partial\Omega_k} D_k\mathbf{u}_k\cdot\overline{\mathbf{v}_k}\,ds = 0,$$

where the matrixes D_k and Z_k are the same as in [17]. Define the matrixes L_k^+ and L_k^- as follows.

$$L_k^+ = \frac{1}{\sqrt{2\sigma}}(-Z_k, \sigma(Z_k)^2) \ \text{ and } \ L_k^- = \frac{1}{\sqrt{2\sigma}}(-Z_k, -\sigma(Z_k)^2)$$

Define $D_k^{\pm} = \pm(L_k^{\pm})^T(L_k^{\pm})$. Then a simple calculation shows that $D_k = D_k^+ + D_k^-$. Using the splitting of D_k and the factorization of each term in the splitting we may rewrite (3.22) as

$$(3.23)\qquad \int_{\partial\Omega_k} (L_k^+\mathbf{u}_k)\cdot\overline{(L_k^+\mathbf{v}_k)} - (L_k^-\mathbf{u}_k)\cdot\overline{(L_k^-\mathbf{v}_k)}\,ds = 0.$$

Note that $Z_k\mathbf{a} = -\mathbf{n}_k\times\mathbf{a}$ for any vector $\mathbf{a}$ and $Z_k = -(Z_k)^T$. Then we have on the interface Γ_{kj}

$$(3.24)\qquad L_k^- = \frac{1}{\sqrt{2\sigma}}(-Z_k, -\sigma(Z_k)^2) = -\frac{1}{\sqrt{2\sigma}}(-Z_j, \sigma(Z_j)^2) = -L_j^+.$$

Using (3.24) and the boundary condition of (3.17), we obtain

$$(3.25)\qquad \begin{cases} L_k^-\mathbf{u}_k = -L_j^+\mathbf{u}_j & on \quad \Gamma_{kj} \\ L_k^-\mathbf{u}_k = QL_k^+\mathbf{u}_k + \hat{\mathbf{g}} & on \quad \partial\Omega_k\cap\gamma, \end{cases}$$

where $\hat{\mathbf{g}} = \frac{\mathbf{g}}{\sqrt{2\sigma}}$. Substituting this into (3.23), and summing on all the elements, we get the desired variational formulation: to find $\mathbf{u}\in\mathbf{U}(\mathcal{T}_h)$, such that

$$(3.26)\qquad \begin{aligned} &\sum_k \int_{\partial\Omega_k} (L_k^+\mathbf{u}_k)\cdot\overline{(L_k^+\mathbf{v}_k)}\,ds + \sum_{k\neq j}\int_{\Gamma_{kj}} (L_j^+\mathbf{u}_j)\cdot\overline{(L_k^-\mathbf{v}_k)}\,ds \\ &-\sum_k\int_{\gamma_k} Q(L_k^+\mathbf{u}_k)\cdot\overline{(L_k^-\mathbf{v}_k)}\,ds = \sum_k\int_{\gamma_k}\hat{\mathbf{g}}\cdot\overline{(L_k^-\mathbf{v}_k)}\,ds, \quad \forall\mathbf{v}\in\mathbf{V}(\mathcal{T}_h). \end{aligned}$$

We can derive the following result as in the proof of Theorem 3.1.

Theorem 3.2. *Let $\mathbf{E},\mathbf{H}\in H(curl;\Omega)$, assume that $Z_k\mathbf{E}, Z_k^2\mathbf{H}\in(L^2(\partial\Omega_k))^3, k = 1,\cdots,N$. Then the reference problem (3.17) is equivalent to the new variational problem (3.26).*

4. Discretization of the variational problems. In this section we introduce discretizations of the variational problems described in the last two sections. The discretization for Helmholtz equations is based on a finite-dimensional trial space $V_p(\mathcal{T}_h) \subset V(\mathcal{T}_h)$ and a finite-dimensional test space $W_p(\mathcal{T}_h) \subset W(\mathcal{T}_h)$. The discretization for Maxwell's equations is based on a finite-dimensional trial space $\mathbf{U}_p(\mathcal{T}_h) \subset \mathbf{U}(\mathcal{T}_h)$ and a finite-dimensional test space $\mathbf{V}_p(\mathcal{T}_h) \subset \mathbf{V}(\mathcal{T}_h)$. We construct the precise definitions of such spaces with which to discretize the VTCR method and the UWVF method.

4.1. The case of Helmholtz equation. In each element Ω_k, we introduce a finite number of functions y_{kl} $(l = 1, 2, \cdots, p)$ supported in Ω_k and that are independent solutions of the homogeneous Helmholtz equation (without boundary condition) in the element Ω_k $(k = 1, 2, \cdots, N)$.

For simplification, we consider some constant number p of basis functions for every elements Ω_k. Particularly, in this paper we will choose y_{kl} as the wave shape functions on Ω_k, which satisfy

$$\begin{cases} y_{kl}(\mathbf{x}) = e^{i\kappa(\mathbf{x}\cdot\boldsymbol{\alpha}_l)}, \quad \mathbf{x} \in \Omega_k, \\ \boldsymbol{\alpha}_l \cdot \boldsymbol{\alpha}_l = 1, \\ l \neq s \to \boldsymbol{\alpha}_l \neq \boldsymbol{\alpha}_s, \end{cases} \tag{4.1}$$

where $\boldsymbol{\alpha}_l$ $(l = 1, \cdots, p)$ are unit wave propagation directions to be specified later.

The basis functions of $V_p(\mathcal{T}_h)$ can be defined as

$$\phi_{kl}(\mathbf{x}) = \begin{cases} y_{kl}(\mathbf{x}), \quad \mathbf{x} \in \Omega_k, \\ 0, \quad \mathbf{x} \in \Omega_j \ \text{ satisfying } \ j \neq k \end{cases} \qquad (k, j = 1, \cdots, N; \ l = 1, \cdots, p). \tag{4.2}$$

Thus the space $V(\mathcal{T}_h)$ is discretized by the subspace

$$V_p(\mathcal{T}_h) = \text{span}\Big\{\phi_{kl} : \ k = 1, \cdots, N; \ l = 1, \cdots, p\Big\}. \tag{4.3}$$

During numerical simulations, the directions of the wave vectors of these wave functions, for two-dimensional problems, are uniformly distributed as follows:

$$\boldsymbol{\alpha}_l = \begin{pmatrix} (cos(2\pi(l-1)/p) \\ sin(2\pi(l-1)/p)) \end{pmatrix} \quad (l = 1, \cdots, p).$$

For three-dimensional problems, we use the optimal spherical codes from [24] to generate the wave propagation derections $\boldsymbol{\alpha}_l$ $(l = 1, \cdots, p)$.

The discrete test space $W_p(\mathcal{T}_h) \subset W(\mathcal{T}_h)$ for the UWVF method is constructed as follows. First, we choose $\tilde{y}_{kl}$ as the wave shape functions on Ω_k, which satisfy

$$\tilde{y}_{kl}(\mathbf{x}) = e^{i\bar{\kappa}(\mathbf{x}\cdot\boldsymbol{\alpha}_l)}, \quad \mathbf{x} \in \Omega_k, \tag{4.4}$$

then the basis functions of $W_p(\mathcal{T}_h)$ can be defined as

$$\xi_{kl}(\mathbf{x}) = \begin{cases} \tilde{y}_{kl}(\mathbf{x}), \quad \mathbf{x} \in \Omega_k, \\ 0, \quad \mathbf{x} \in \Omega_j \ \text{ satisfying } \ j \neq k \end{cases} \qquad (k, j = 1, \cdots, N; \ l = 1, \cdots, p). \tag{4.5}$$

4.2. The case of Maxwell's equations. In practice, following [3], a suitable family of plane waves, which are solutions of the constant-coefficient Maxwell equations, are generated on Ω_k by choosing p unit propagation directions $\mathbf{d}_l$, $l = 1, \cdots, p$ (we use the optimal spherical codes from [24]), and defining a real unit polarization vector $\mathbf{G}_l$ orthogonal to $\mathbf{d}_l$. By using such propagation directions and polarization vectors, we can define the complex polarization vectors $\mathbf{F}_l$ and $\mathbf{F}_{l+p}$ as

$$\mathbf{F}_l = \mathbf{G}_l + \mathrm{i}\mathbf{G}_l \times \mathbf{d}_l, \quad \mathbf{F}_{l+p} = \mathbf{G}_l - \mathrm{i}\mathbf{G}_l \times \mathbf{d}_l \quad (l = 1, \cdots, p).$$

Notice that the complex polarization vectors are the same as in [5, 17], but differ slightly from those in [13]. We then define the complex functions $\begin{pmatrix} \mathbf{E}_l \\ \mathbf{H}_l \end{pmatrix}$:

$$\text{(4.6)} \qquad \begin{cases} \mathbf{E}_l = \sqrt{\mu}\,\mathbf{F}_l \exp(\mathrm{i}\kappa \mathbf{d}_l \cdot \mathbf{x}) \\ \mathbf{H}_l = i\sqrt{\varepsilon}\,\mathbf{F}_l \exp(\mathrm{i}\kappa \mathbf{d}_l \cdot \mathbf{x}) \end{cases} \quad \text{and} \quad \begin{cases} \mathbf{E}_{l+p} = \sqrt{\mu}\,\mathbf{G}_l \exp(\mathrm{i}\kappa \mathbf{d}_l \cdot \mathbf{x}) \\ \mathbf{H}_{l+p} = -i\sqrt{\varepsilon}\,\mathbf{G}_l \exp(\mathrm{i}\kappa \mathbf{d}_l \cdot \mathbf{x}), \end{cases}$$

where $\kappa = \omega\sqrt{\varepsilon\mu}$, $l = 1, \cdots, p$. It is easy to verify that every functions $\begin{pmatrix} \mathbf{E}_l \\ \mathbf{H}_l \end{pmatrix}$ $(l = 1, \cdots, 2p)$ satisfy the homogeneous Maxwell's system (2.14).

Let Q_{2p} denote the space spanned by the $2p$ plane wave functions $\begin{pmatrix} \mathbf{E}_l \\ \mathbf{H}_l \end{pmatrix}$ $(l = 1, \cdots, 2p)$. Define the discrete trial plane wave space

$$\text{(4.7)} \qquad \mathbf{U}_p(\mathcal{T}_h) = \left\{ \mathbf{v} \in L^2(\Omega) : \ \mathbf{v}|_K \in Q_{2p} \ \text{ for any } \ K \in \mathcal{T}_h \right\}.$$

The discrete test space $\mathbf{V}_p(\mathcal{T}_h) \subset \mathbf{V}(\mathcal{T}_h)$ for the UWVF method is constructed by choosing $\begin{pmatrix} \boldsymbol{\xi}_l \\ \psi_l \end{pmatrix}$ $(l = 1, \cdots, 2p)$ as the wave shape basis functions on Ω_k, which satisfy

$$\text{(4.8)} \qquad \begin{cases} \boldsymbol{\xi}_l = \sqrt{\mu}\,\mathbf{F}_l \exp(\mathrm{i}\bar{\kappa} \mathbf{d}_l \cdot \mathbf{x}) \\ \psi_l = i\sqrt{\bar{\varepsilon}}\,\mathbf{F}_l \exp(\mathrm{i}\bar{\kappa} \mathbf{d}_l \cdot \mathbf{x}) \end{cases} \quad \text{and} \quad \begin{cases} \boldsymbol{\xi}_{l+p} = \sqrt{\mu}\,\mathbf{G}_l \exp(\mathrm{i}\bar{\kappa} \mathbf{d}_l \cdot \mathbf{x}) \\ \psi_{l+p} = -i\sqrt{\bar{\varepsilon}}\,\mathbf{G}_l \exp(\mathrm{i}\bar{\kappa} \mathbf{d}_l \cdot \mathbf{x}). \end{cases}$$

5. Nonhomogeneous Helmholtz and Maxwell's equations. The VTCR method in Section 2 and the UWVF method in Section 3 were described only for the homogeneous Helmholtz equation and Maxwell equations. Recently, a PWLS method (see [15]) and a PWLS-LSFE method (see [16]) were proposed for discretization of nonhomogeneous harmonic Helmholtz and Maxwell's equations. As pointed out in [16], for the PWLS-LSFE method, a plane wave method combined with local spectral elements for discretization of the nonhomogeneous Helmholtz equation and time-harmonic Maxwell equations was introduced and error estimates of the resulting approximate solutions were derived. The error estimates show that the approximate solutions generated by the PWLS-LSFE method possess high accuracy and the numerical results indicate that the approximation generated by the PWLS-LSFE method is much more accurate than that generated by the original method proposed in [15]. In this section, combined with the local spectral elements (see [16]), we propose another way to discretize the nonhomogeneous Helmholtz and Maxwell equations that involves using the VTCR method and UWVF method, respectively.

5.1. The VTCR method combined with local spectral element. In this subsection, we design the VTCR method combined with local spectral element for solving Nonhomogeneous Helmholtz and Maxwell's equations. For convenience, we call the method as VTCR-LSFE method.

5.1.1. The case of nonhomogeneous Helmholtz equation. Consider the nonhomogeneous Helmholtz equation

$$\left\{\begin{array}{rcll} -\Delta u - \kappa^2 u & = & f & \text{in} \quad \Omega, \\ u & = & g_d & \text{on} \quad \gamma_d, \\ \frac{\partial u}{\partial \mathbf{n}} & = & g_n & \text{on} \quad \gamma_n, \\ \frac{\partial u}{\partial \mathbf{n}} + i\kappa u & = & g_r & \text{on} \quad \gamma_r, \end{array}\right. \tag{5.1}$$

where $f \in L^2(\Omega)$.

As in [16], the basic idea is to decompose the solution u of (5.1) into

$$u = u^{(1)} + u^{(2)}, \tag{5.2}$$

where $u^{(1)}$ is a particular solution of (5.1) without the primal boundary condition, and $u^{(2)}$ satisfies a locally homogeneous Helmholtz equation. Without loss of generality, we assume that the function f is well defined in a slightly large domain containing Ω as its subdomain (otherwise, we can build a stable extension of f).

For each element Ω_k, let Ω_k^* be a fictitious domain that has almost the same size with Ω_k and contains Ω_k as its subdomain. Let $u^{(1)} \in L^2(\Omega)$ be defined as $u^{(1)}\mid_{\Omega_k} = u_k^{(1)}\mid_{\Omega_k}$ for each Ω_k, where $u_k^{(1)} \in H^1(\Omega_k^*)$ satisfies the *local* nonhomogeneous Helmholtz equation on the fictitious domain Ω_k^*:

$$\left\{\begin{array}{lll} -\Delta u_k^{(1)} - \kappa^2 u_k^{(1)} = f & \text{in} & \Omega_k^* \\ (\partial_{\mathbf{n}_k} + i\kappa) u_k^{(1)} = 0 & \text{on} & \partial\Omega_k^* \end{array}\right. \quad (k = 1, 2, \ldots, N). \tag{5.3}$$

The variational problem of (5.3) is to find $u_k^{(1)} \in H^1(\Omega_k^*)$ such that

$$\left\{\begin{array}{l} \int_{\Omega_k^*} (\nabla u_k^{(1)} \cdot \nabla \bar{v}_k - \kappa^2 u_k^{(1)} \bar{v}_k) d\mathbf{x} + \int_{\partial\Omega_k^*} i\kappa u_k^{(1)} \bar{v}_k d\mathbf{x} = \int_{\Omega_k^*} f \bar{v}_k d\mathbf{x}, \\ \qquad\qquad \forall v_k \in H^1(\Omega_k^*) \ (k = 1, 2, \ldots, N). \end{array}\right. \tag{5.4}$$

Let q be a positive integer and D be a bounded and connected domain in $\mathbb{R}^n$. Let $S_q(D)$ denote the set of polynomials defined on D, whose orders are less or equal to q. Set $\mathbf{S}_q(D) = (S_q(D))^3$. Define the approximate solutions u_h as follows:

$$u_h = u_h^{(1)} + u_h^{(2)} \tag{5.5}$$

where $u_h^{(1)} \in \prod_{k=1}^N S_q(\Omega_k^*)$ and $u_h^{(2)} \in V_p(\mathcal{T}_h)$.

The discrete variational problems of (5.4) are: to find $u_{k,h}^{(1)} = u_h^{(1)}|_{\Omega_k^*} \in S_q(\Omega_k^*)$ such that

$$\left\{\begin{array}{l} \int_{\Omega_k^*} (\nabla u_{k,h}^{(1)} \cdot \nabla \bar{v}_k - \kappa^2 u_{k,h}^{(1)} \bar{v}_k) \, d\boldsymbol{x} + \int_{\partial\Omega_k^*} i\kappa u_{k,h}^{(1)} \bar{v}_k \, ds = \int_{\Omega_k^*} f \bar{v}_k \, d\boldsymbol{x}, \\ \qquad\qquad \forall v_k \in S_q(\Omega_k^*) \ (k = 1, 2, \ldots, N). \end{array}\right. \tag{5.6}$$

In this paper we choose the fictitious domain Ω_k^* to be the disc (for the two-dimensional case) or the sphere (for the three-dimensional case) described in [16, Sec. 3].

It is easy to see that $u^{(2)} = u - u^{(1)}$ is uniquely determined by the following homogeneous Helmholtz equations of $u_k^{(2)} = u^{(2)}\mid_{\Omega_k}$:

$$-\Delta u_k^{(2)} - \kappa^2 u_k^{(2)} = 0 \quad \text{in} \quad \Omega_k \ (k = 1, 2, \ldots, N), \tag{5.7}$$

with the following boundary condition on γ and the interface conditions on Γ_{kj}:

$$(5.8)\quad \begin{cases} u_k^{(2)} = g_d - u_k^{(1)} & \text{over} \quad \gamma_d, \\ \partial_{\mathbf{n}} u_k^{(2)} = g_n - \partial_{\mathbf{n}} u_k^{(1)} & \text{over} \quad \gamma_n, \\ (\partial_{\mathbf{n}} + i\kappa) u_k^{(2)} = g - (\partial_{\mathbf{n}} + i\kappa) u_k^{(1)} & \text{over} \quad \gamma_r, \quad (k \neq j;\ k, j = 1, 2, \cdots, N). \\ u_k^{(2)} - u_j^{(2)} = -(u_k^{(1)} - u_j^{(1)}) & \text{over} \quad \Gamma_{kj}, \\ \partial_{\mathbf{n}_k} u_k^{(2)} + \partial_{\mathbf{n}_j} u_j^{(2)} = -(\partial_{\mathbf{n}_k} u_k^{(1)} + \partial_{\mathbf{n}_j} u_j^{(1)}) & \text{over} \quad \Gamma_{kj} \end{cases}$$

According to the idea of the VTCR method described in Section 2, the variational problem of (5.7)-(5.8) is: to find $u^{(2)} \in V(\mathcal{T}_h)$ such that

(5.9)

$$\begin{aligned} & Re\Big\{ \int_{\gamma_d} u_k^{(2)} \cdot \overline{i\partial_{\mathbf{n}} v}\, ds + \int_{\gamma_n} \overline{i\partial_{\mathbf{n}} u_k^{(2)}} \cdot v\, ds \\ & + \int_{\gamma_r} \frac{1}{2}\Big((\partial_{\mathbf{n}} + i\kappa) u_k^{(2)} \cdot \overline{\frac{-1}{\overline{\kappa}} \partial_{\mathbf{n}} v} + \overline{i\Big((\partial_{\mathbf{n}} + i\kappa) u_k^{(2)}\Big) \cdot v} \Big)\, ds \\ & + \sum_{j \neq k} \frac{1}{2} \int_{\Gamma_{kj}} \Big((u_k^{(2)} - u_j^{(2)}) \cdot \overline{i(\partial_{\mathbf{n}_k} v_k - \partial_{\mathbf{n}_j} v_j)} + \overline{i(\partial_{\mathbf{n}_k} u_k^{(2)} + \partial_{\mathbf{n}_j} u_j^{(2)})} \cdot (v_k + v_j) \Big)\, ds \Big\} \\ & = Re\Big\{ \int_{\gamma_d} (g_d - u_k^{(1)}) \cdot \overline{i\partial_{\mathbf{n}} v}\, ds + \int_{\gamma_n} \overline{i(g_n - \partial_{\mathbf{n}} u_k^{(1)})} \cdot v\, ds \\ & + \int_{\gamma_r} \frac{1}{2}\Big(\Big(g_r - (\partial_{\mathbf{n}} + i\kappa) u_k^{(1)}\Big) \cdot \overline{\frac{-1}{\overline{\kappa}} \partial_{\mathbf{n}} v} + \overline{i\Big(g_r - (\partial_{\mathbf{n}} + i\kappa) u_k^{(1)}\Big) \cdot v} \Big)\, ds \; - \\ & \sum_{j \neq k} \frac{1}{2} \int_{\Gamma_{kj}} \Big((u_k^{(1)} - u_j^{(1)}) \cdot \overline{i(\partial_{\mathbf{n}_k} v_k - \partial_{\mathbf{n}_j} v_j)} + \overline{i(\partial_{\mathbf{n}_k} u_k^{(1)} + \partial_{\mathbf{n}_j} u_j^{(1)})} \cdot (v_k + v_j) \Big)\, ds \Big\}, \forall v \in V(\mathcal{T}_h). \end{aligned}$$

In this case, the discrete variational problem associated with (5.9) can be described as follows: to find $u_h^{(2)} \in V_p(\mathcal{T}_h)$ such that $u_h^{(2)}$ satisfy (5.9) for $\forall v_h \in V_p(\mathcal{T}_h)$.

5.1.2. The case of nonhomogeneous Maxwell's equations. Consider the nonhomogeneous Maxwell equations

$$(5.10)\qquad \begin{cases} \nabla \times \mathbf{E} - i\omega\mu \mathbf{H} = 0 \\ \nabla \times \mathbf{H} + i\omega\varepsilon \mathbf{E} = \mathbf{J} \end{cases} \quad in \quad \Omega$$

with the boundary condition (2.13). We need to transform nonhomogeneous problems into homogeneous problems to use the VTCR method introduced in Section 2.

Similar to the case of Helmholtz equation, we assume that $\mathbf{J}$ is well defined in a sufficiently large domain containing Ω as its subdomain and decompose the solution $\mathbf{E}$ of the problem (2.12) into $\mathbf{E} = \mathbf{E}^{(1)} + \mathbf{E}^{(2)}$, where $\mathbf{E}^{(1)}$ is a particular solution of (2.12) without the primal boundary condition, and $\mathbf{E}^{(2)}$ locally satisfies homogeneous Maxwell's equations.

For each element Ω_k, let Ω_k^* be the fictitious domain described in the last subsection. The particular solution $\mathbf{E}^{(1)} \in (L^2(\Omega))^3$ is defined as $\mathbf{E}^{(1)}\ |_{\Omega_k} = \mathbf{E}_k^{(1)}\ |_{\Omega_k}$ for each Ω_k, where $\mathbf{E}_k^{(1)} \in H(\text{curl}; \Omega_k^*)$ satisfies the nonhomogeneous *local* Maxwell equations on the fictitious domain Ω_k^*:

$$(5.11)\qquad \nabla \times \Big(\frac{1}{i\omega\mu} \nabla \times \mathbf{E}_k^{(1)}\Big) + i\omega\varepsilon \mathbf{E}_k^{(1)} = \mathbf{J} \quad \text{in} \quad \Omega_k^*\ (k = 1, 2, \ldots, N)$$

with the homogeneous boundary condition

$$-\mathbf{E}_k^{(1)} \times \mathbf{n} + \frac{\sigma}{i\omega\mu}(\nabla \times \mathbf{E}_k^{(1)}) \times \mathbf{n} \times \mathbf{n} = 0 \quad \text{on} \quad \partial\Omega_k^*. \tag{5.12}$$

The variational problem of (5.11) − (5.12) is to find $\mathbf{E}_k^{(1)} \in H(\mathrm{curl}, \Omega_k^*)$ such that

$$\begin{cases} \int_{\Omega_k^*} (\frac{1}{i\omega\mu}\nabla \times \mathbf{E}_k^{(1)} \cdot \nabla \times \bar{\mathbf{F}}_k + i\omega\varepsilon\mathbf{E}_k^{(1)} \cdot \bar{\mathbf{F}}_k)\, d\boldsymbol{x} + \int_{\partial\Omega_k^*} \frac{1}{\sigma}(\mathbf{E}_k^{(1)} \times \mathbf{n}) \times \mathbf{n} \cdot \bar{\mathbf{F}}_k\, ds \\ \qquad = \int_{\Omega_k^*} \mathbf{J} \cdot \bar{\mathbf{F}}_k\, d\boldsymbol{x}, \qquad \forall \mathbf{F}_k \in \mathrm{H}(\mathrm{curl}, \Omega_k^*)\ (k = 1, 2, \ldots, N). \end{cases} \tag{5.13}$$

When $\mathbf{J}$ satisfies $\mathbf{J} \in (L^2(\Omega_k^*))^3$, the variational problem (5.13) possesses a unique solution $\mathbf{E}_k^{(1)} \in H(\mathrm{curl}, \Omega_k^*)$ (see [20, Chap 4]).

Set the corresponding particular solution $\mathbf{H}^{(1)} \in (L^2(\Omega))^3$ which is defined as $\mathbf{H}^{(1)}\mid_{\Omega_k} = \mathbf{H}_k^{(1)}\mid_{\Omega_k}$ for each Ω_k, where $\mathbf{H}_k^{(1)} = \frac{1}{i\omega\mu}\nabla \times \mathbf{E}_k^{(1)} \in H(\mathrm{curl}; \Omega_k^*)$.

It is easy to see that $\begin{pmatrix} \mathbf{E}^{(2)} \\ \mathbf{H}^{(2)} \end{pmatrix} = \begin{pmatrix} \mathbf{E} - \mathbf{E}^{(1)} \\ \mathbf{H} - \mathbf{H}^{(1)} \end{pmatrix}$ is uniquely determined by the following homogeneous Maxwell equations of $\begin{pmatrix} \mathbf{E}_k^{(2)} \\ \mathbf{H}_k^{(2)} \end{pmatrix} = \begin{pmatrix} \mathbf{E}^{(2)}\mid_{\Omega_k} \\ \mathbf{H}^{(2)}\mid_{\Omega_k} \end{pmatrix}$:

$$\begin{cases} \nabla \times \mathbf{E}_k^{(2)} - i\omega\mu\mathbf{H}_k^{(2)} = 0 \\ \nabla \times \mathbf{H}_k^{(2)} + i\omega\varepsilon\mathbf{E}_k^{(2)} = 0 \end{cases} \quad in \quad \Omega_k\ (k = 1, 2, \ldots, N), \tag{5.14}$$

with the following boundary condition on γ and the interface conditions on Γ_{kj} $(k < j;\ k, j = 1, \ldots, N)$:

(5.15)

$$\begin{cases} -\mathbf{E}_k^{(2)} \times \mathbf{n}_k = \mathbf{g}_d - (-\mathbf{E}_k^{(1)} \times \mathbf{n}_k) & \text{on} \quad \gamma_{d,k} = \gamma_d \cap \partial\Omega_k, \\ \mathbf{H}_k^{(2)} \times \mathbf{n}_k \times \mathbf{n}_k = \mathbf{g}_n - \mathbf{H}_k^{(1)} \times \mathbf{n}_k \times \mathbf{n}_k & \text{on} \quad \gamma_{n,k} = \gamma_n \cap \partial\Omega_k, \\ -\mathbf{E}_k^{(2)} \times \mathbf{n}_k + \sigma(\mathbf{H}_k^{(2)} \times \mathbf{n}_k) \times \mathbf{n}_k = \mathbf{g}_r - (-\mathbf{E}_k^{(1)} \times \mathbf{n}_k + \sigma(\mathbf{H}_k^{(1)} \times \mathbf{n}_k) \times \mathbf{n}_k) & \text{on} \quad \gamma_{r,k} = \gamma_r \cap \partial\Omega_k, \\ \mathbf{E}_k^{(2)} \times \mathbf{n}_k^{(2)} + \mathbf{E}_j \times \mathbf{n}_j = -(\mathbf{E}_k^{(1)} \times \mathbf{n}_k + \mathbf{E}_j^{(1)} \times \mathbf{n}_j) & \text{over} \quad \Gamma_{kj}, \\ \mathbf{H}_k^{(2)} \times \mathbf{n}_k + \mathbf{H}_j^{(2)} \times \mathbf{n}_j = -(\mathbf{H}_k^{(1)} \times \mathbf{n}_k + \mathbf{H}_j^{(1)} \times \mathbf{n}_j) & \text{over} \quad \Gamma_{kj}, \\ & (k < j;\ k, j = 1, 2, \ldots, N). \end{cases}$$

The variational problem of (5.14)-(5.15) is: to find $\begin{pmatrix}\mathbf{E}^{(2)}\\ \mathbf{H}^{(2)}\end{pmatrix}$ such that

$$
\begin{aligned}
(5.16)\quad & Re\Big\{\sum_{k=1}^{N}\int_{\gamma_{d,k}}(-\mathbf{E}_k^{(2)}\times\mathbf{n})\cdot\overline{i\boldsymbol{\xi}\times\mathbf{n}\times\mathbf{n}}\,ds+\sum_{k=1}^{N}\int_{\gamma_{n,k}}\overline{i(\mathbf{H}_k^{(2)}\times\mathbf{n}\times\mathbf{n})}\cdot(-\boldsymbol{\psi}\times\mathbf{n})\,ds\\
&+\sum_{k=1}^{N}\int_{\gamma_{r,k}}\frac{1}{2}\Big(\Big(-\mathbf{E}_k^{(2)}\times\mathbf{n}+\sigma(\mathbf{H}_k^{(2)}\times\mathbf{n})\times\mathbf{n}\Big)\cdot\overline{i\boldsymbol{\xi}\times\mathbf{n}\times\mathbf{n}}\\
&+\overline{i\Big(-\mathbf{E}_k^{(2)}\times\mathbf{n}+\sigma(\mathbf{H}_k^{(2)}\times\mathbf{n})\times\mathbf{n}\Big)}\cdot\frac{1}{\sigma}(-\boldsymbol{\psi}\times\mathbf{n})\Big)\,ds\\
&+\sum_{j\neq k}\frac{1}{2}\int_{\Gamma_{kj}}\Big((-\mathbf{E}_k^{(2)}\times\mathbf{n}_k-\mathbf{E}_j^{(2)}\times\mathbf{n}_j)\cdot\overline{i\Big((\boldsymbol{\xi}_k\times\mathbf{n}_k)\times\mathbf{n}_k+(\boldsymbol{\xi}_j\times\mathbf{n}_j)\times\mathbf{n}_j\Big)}\\
&+\overline{i\Big((\boldsymbol{H}_k^{(2)}\times\mathbf{n}_k)\times\mathbf{n}_k-(\boldsymbol{H}_j^{(2)}\times\mathbf{n}_j)\times\mathbf{n}_j\Big)}\cdot(-\boldsymbol{\psi}_k\times\mathbf{n}_k+\boldsymbol{\psi}_j\times\mathbf{n}_j)\Big)\,ds\Big\}
\end{aligned}
$$

$$
\begin{aligned}
=\ & Re\Big\{\sum_{k=1}^{N}\int_{\gamma_{d,k}}(\mathbf{g}_d+\mathbf{E}_k^{(1)}\times\mathbf{n})\cdot\overline{i\boldsymbol{\xi}\times\mathbf{n}\times\mathbf{n}}ds+\sum_{k=1}^{N}\int_{\gamma_{n,k}}\overline{i(\mathbf{g}_n-\mathbf{H}_k^{(1)}\times\mathbf{n}\times\mathbf{n})}\cdot(-\boldsymbol{\psi}\times\mathbf{n})\,ds\\
&+\sum_{k=1}^{N}\int_{\gamma_{r,k}}\frac{1}{2}\Big(\Big(\mathbf{g}_r-(-\mathbf{E}_k^{(1)}\times\mathbf{n}+\sigma(\mathbf{H}_k^{(1)}\times\mathbf{n})\times\mathbf{n})\Big)\cdot\overline{i\boldsymbol{\xi}\times\mathbf{n}\times\mathbf{n}}\\
&+\overline{i\Big(\mathbf{g}_r-(-\mathbf{E}_k^{(1)}\times\mathbf{n}+\sigma(\mathbf{H}_k^{(1)}\times\mathbf{n})\times\mathbf{n})\Big)}\cdot\frac{1}{\sigma}(-\boldsymbol{\psi}\times\mathbf{n})\Big)\,ds\\
&+\sum_{j\neq k}\frac{1}{2}\int_{\Gamma_{kj}}\Big((-\mathbf{E}_k^{(1)}\times\mathbf{n}_k-\mathbf{E}_j^{(1)}\times\mathbf{n}_j)\cdot\overline{i\Big((\boldsymbol{\xi}_k\times\mathbf{n}_k)\times\mathbf{n}_k+(\boldsymbol{\xi}_j\times\mathbf{n}_j)\times\mathbf{n}_j\Big)}\\
&+\overline{i\Big((\boldsymbol{H}_k^{(1)}\times\mathbf{n}_k)\times\mathbf{n}_k-(\boldsymbol{H}_j^{(1)}\times\mathbf{n}_j)\times\mathbf{n}_j\Big)}\cdot(-\boldsymbol{\psi}_k\times\mathbf{n}_k+\boldsymbol{\psi}_j\times\mathbf{n}_j)\Big)\,ds\Big\},\ \forall(\boldsymbol{\psi},\boldsymbol{\xi})\in\mathbf{V}(\mathcal{T}_h).
\end{aligned}
$$

The cost of the solution of the above problem is same as that of the homogeneous Maxwell's equations.

5.2. The UWVF method. In this subsection, we design the UWVF method combined with local spectral element for solving Nonhomogeneous Helmholtz and Maxwell's equations. For convenience, we call the method as UWVF-LSFE method.

5.2.1. The case of nonhomogeneous Helmholtz equation. Consider the nonhomogeneous Helmholtz equation

$$
(5.17)\qquad \left\{\begin{array}{rcll} -\Delta u-\kappa^2 u &=& f & \text{in}\ \ \Omega,\\ \frac{\partial u}{\partial \mathbf{n}}+i\kappa u &=& g & \text{on}\ \ \gamma. \end{array}\right.
$$

As described in subsubsection 5.1.1, the basic idea is to decompose the solution u of (5.1) into

$$
(5.18)\qquad u=u^{(1)}+u^{(2)},
$$

where $u^{(1)}$ is the solution of (5.4), and $u^{(2)}$ satisfies a locally homogeneous Helmholtz equation (5.7) with the following boundary condition on γ and the interface conditions on Γ_{kj}:

$$(5.19)\quad \begin{cases} (\partial_{\mathbf{n}_k} + i\kappa)u^{(2)}|_{\Gamma_{kj}} = (-\partial_{\mathbf{n}_j} + i\kappa)u^{(2)}|_{\Gamma_{jk}} + (-\partial_{\mathbf{n}_j} + i\kappa)u^{(1)}|_{\Gamma_{jk}} - (\partial_{\mathbf{n}_k} + i\kappa)u^{(1)}|_{\Gamma_{kj}}, \\ (\partial_{\mathbf{n}_k} + i\kappa)u^{(2)}|_{\gamma_k} = -(\partial_{\mathbf{n}_k} + i\kappa)u^{(1)}|_{\gamma_k} + g. \end{cases}$$

According to the idea of the UWVF method described in Section 3, the variational problem of (5.7) and (5.19) is: to find $u^{(2)} \in V(\mathcal{T}_h)$ defined by such that

(5.20)

$$\sum_k \int_{\partial\Omega_k} (-\partial_{\mathbf{n}_k} + i\kappa)u_k^{(2)}\, \overline{(-\partial_{\mathbf{n}_k} + i\,\overline{\kappa}\,)e_k}\, ds - \sum_{k\neq j} \int_{\Gamma_{kj}} (-\partial_{\mathbf{n}_j} + i\kappa)u_j^{(2)}\, \overline{(\partial_{\mathbf{n}_k} + i\,\overline{\kappa}\,)e_k}\, ds$$
$$= \sum_k \int_{\gamma_k} g\, \overline{(\partial_{\mathbf{n}_k} + i\,\overline{\kappa}\,)e_k}\, ds + \sum_{k\neq j} \int_{\Gamma_{kj}} (-\partial_{\mathbf{n}_j} + i\kappa)u_j^{(1)}\, \overline{(\partial_{\mathbf{n}_k} + i\,\overline{\kappa}\,)e_k}\, ds -$$
$$\Big(\sum_{k\neq j} \int_{\Gamma_{kj}} (\partial_{\mathbf{n}_k} + i\kappa)u_k^{(1)}\, \overline{(\partial_{\mathbf{n}_k} + i\,\overline{\kappa}\,)e_k}\, ds + \sum_k \int_{\gamma_k} (\partial_{\mathbf{n}_k} + i\kappa)u_k^{(1)}\, \overline{(\partial_{\mathbf{n}_k} + i\,\overline{\kappa}\,)e_k}\, ds\Big),\quad \forall e \in W(\mathcal{T}_h).$$

Similar to the subsection 5.1.1, the numerical approximate solutions u_h can be decomposed into

$$(5.21)\qquad u_h = u_h^{(1)} + u_h^{(2)},$$

where $u_h^{(1)} \in \prod_{k=1}^N S_q(\Omega_k^*)$ satisfy (5.6) and $u_h^{(2)} \in V_p(\mathcal{T}_h)$ satisfy (5.20) for $\forall e_h \in W_p(\mathcal{T}_h)$.

5.2.2. Error estimates of the approximation solutions. Since the trial function space is different from the test function space for the case of complex wavenumbers κ, the new variant of the UWVF method is essentially a discontinuous Petrov-Galerkin method. It is difficult to prove that the bilinear form meets the inf-sup condition, thus in this subsubsection we derive error estimates of the approximate solutions u_h defined in the last section for the particular case of real wavenumbers κ only, where the UWVF method is a standard discontinuous Galerkin mehtod.

Let s and m be given positive integers satisfying $m \geq 2s + 1$. Let the number p of plane wave propagation directions be chosen as $p = (2m + 1)$ in 2D and $p = (m + 1)^2$ in 3D, respectively. Since each element Ω_k is convex, it is star-shaped with respect to a ball.

As in [19], for a bounded and connected domain $D \subset \Omega$, let $\|\cdot\|_{s,\kappa,D}$ be the $\kappa-$weighted Sobolev norm defined by

$$\|v\|_{s,\kappa,D} = \sum_{j=0}^{s} \kappa^{2(s-j)}|v|_{j,D}^2.$$

It turns out that the UWVF can be recast as a special plane wave discontinuous galerkin method as pointed out in [9]. Let $\|\cdot\|_{\mathcal{F}_h}$ and $\|\cdot\|_{\mathcal{F}_h^+}$ be the energy norm defined in (3.1) and (3.2) from [12] for the case of $\alpha = \beta = \delta = \frac{1}{2}$, respectively.

The following lemma is a direct consequence of Theorem 4.3 in [16].

LEMMA 5.1. *Let $q \geq 2$ and $2 \leq s \leq q + 1$. Assume that $c_0 \leq \kappa h \leq C_0$ and $f \in H^{s-2}(\Omega_\delta)$. Then the following error estimates hold*

$$(5.22)\qquad (\sum_{k=1}^{N} \|u^{(1)} - u_h^{(1)}\|_{j,\Omega_k}^2)^{\frac{1}{2}} \leq C(\frac{h}{q})^{s-j} \sum_{l=0}^{s-2} \kappa^{s-l-2}\|f\|_{H^l(\Omega_\delta)} \quad (j = 0, 1, 2)$$

and

$$\|u^{(1)} - u_h^{(1)}\|_{\mathcal{F}_h} \le C(1 + \frac{\kappa^2 h^2}{q^2})^{\frac{1}{2}} (\frac{h}{q})^{s-\frac{3}{2}} \sum_{l=0}^{s-2} \kappa^{s-l-\frac{5}{2}} \|f\|_{H^l(\Omega_\delta)}, \tag{5.23}$$

where Ω_δ defined in [16, Sec.4.1.1] is the union of Ω and the boundary layer with the thickness δ, and c_0, C_0 are the constants.

The following approximation can be viewed as a version of Theorem 4.5 in [16].

Lemma 5.2. *Let $q \ge 2$, $2 < s \le \min\{\frac{m+1}{2}, q+1\}$ and $\kappa h = O(1)$. Assume that $f \in H^{s-2}(\Omega_\delta)$ and $u \in H^s(\Omega)$. Then*

$$\|u^{(2)} - u_h^{(2)}\|_{\mathcal{F}_h} \le C\kappa^{-\frac{1}{2}} h^{s-\frac{3}{2}} \max\{m^{-\lambda(s-1-\varepsilon)+\frac{\delta_\lambda}{2}}, q^{-(s-\frac{3}{2})}\} \left(\|u\|_{s,\kappa,\Omega} + \sum_{l=0}^{s-2} \kappa^{s-l-2} \|f\|_{H^l(\Omega_\delta)} \right), \tag{5.24}$$

where $\lambda > 0$ is a constant depending only on the shape of the elements (in particular, $\lambda = 1$ for the case of two dimensions), $\delta_\lambda = \max\{2\lambda - 1, 1\}$, and $\varepsilon = \varepsilon(m) \in (0,1)$ satisfies $\varepsilon(m) \to 0^+$ when $m \to +\infty$.

Proof. Define

$$A(w, v) = \sum_k \int_{\partial\Omega_k} (-\partial_{\mathbf{n}_k} + i\kappa) w_k \overline{(-\partial_{\mathbf{n}_k} + i\,\kappa\,) v_k}\, ds, \tag{5.25}$$

$$B(w, v) = \sum_{k \ne j} \int_{\Gamma_{kj}} (-\partial_{\mathbf{n}_j} + i\kappa) w_j \overline{(\partial_{\mathbf{n}_k} + i\,\kappa\,) v_k}\, ds, \tag{5.26}$$

$$l(v) = \sum_k \int_{\gamma_k} g\, \overline{(\partial_{\mathbf{n}_k} + i\,\kappa\,) v_k}\, ds, \tag{5.27}$$

and

$$C(u, v) = \sum_k \int_{\partial\Omega_k} (\partial_{\mathbf{n}_k} + i\kappa) w_k \overline{(\partial_{\mathbf{n}_k} + i\,\kappa\,) v_k}\, ds. \tag{5.28}$$

Then we get

$$A(u^{(2)}, v^{(2)}) - B(u^{(2)}, v^{(2)}) = l(v^{(2)}) + B(u^{(1)}, v^{(2)}) - C(u^{(1)}, v^{(2)}) \tag{5.29}$$

and

$$A(u_h^{(2)}, v_h^{(2)}) - B(u_h^{(2)}, v_h^{(2)}) = l(v_h^{(2)}) + B(u_h^{(1)}, v_h^{(2)}) - C(u_h^{(1)}, v_h^{(2)}). \tag{5.30}$$

From (5.29) and (5.30), we have

$$A(u^{(2)} - u_h^{(2)}, v_h^{(2)}) - B(u^{(2)} - u_h^{(2)}, v_h^{(2)}) = B(u^{(1)} - u_h^{(1)}, v_h^{(2)}) - C(u^{(1)} - u_h^{(1)}, v_h^{(2)}). \tag{5.31}$$

Let Q_h be the operator defined in Lemma 4.4 from [16]. It follows by (5.31) that

$$\begin{aligned} &A(u^{(2)} - u_h^{(2)}, Q_h u^{(2)} - u_h^{(2)}) - B(u^{(2)} - u_h^{(2)}, Q_h u^{(2)} - u_h^{(2)}) = \\ &B(u^{(1)} - u_h^{(1)}, Q_h u^{(2)} - u_h^{(2)}) - C(u^{(1)} - u_h^{(1)}, Q_h u^{(2)} - u_h^{(2)}). \end{aligned} \tag{5.32}$$

By the bilinear form $\mathcal{A}_h(\cdot,\cdot)$ defined in [9, 12], we can deduce that

$$A(w,v) - B(w,v) = -\mathcal{A}_h(w,v). \tag{5.33}$$

Then, by the direct manipulation, we can deduce that

$$\begin{aligned}
&\|u^{(2)} - u_h^{(2)}\|^2_{\mathcal{F}_h} = \mathrm{Im}\,\mathcal{A}_h(u^{(2)} - u_h^{(2)}, u^{(2)} - u_h^{(2)}) = \\
&\mathrm{Im}\Big\{ - A(u^{(2)} - u_h^{(2)}, u^{(2)} - u_h^{(2)}) + B(u^{(2)} - u_h^{(2)}, u^{(2)} - u_h^{(2)})\Big\} \\
&= \mathrm{Im}\Big\{ - A(u^{(2)} - u_h^{(2)}, u^{(2)} - Q_h u^{(2)}) + B(u^{(2)} - u_h^{(2)}, u^{(2)} - Q_h u^{(2)}) \\
&- B(u^{(1)} - u_h^{(1)}, Q_h u^{(2)} - u_h^{(2)}) + C(u^{(1)} - u_h^{(1)}, Q_h u^{(2)} - u_h^{(2)})\Big\} \\
&= \mathrm{Im}\Big\{\mathcal{A}_h(u^{(2)} - u_h^{(2)}, u^{(2)} - Q_h u^{(2)}) - B(u^{(1)} - u_h^{(1)}, Q_h u^{(2)} - u_h^{(2)}) + \\
&C(u^{(1)} - u_h^{(1)}, Q_h u^{(2)} - u_h^{(2)})\Big\}.
\end{aligned} \tag{5.34}$$

By the proposition 3.5 in [12] and the definition of $\|\cdot\|_{\mathcal{F}_h^+}$, we have

$$\begin{aligned}
&\|u^{(2)} - u_h^{(2)}\|^2_{\mathcal{F}_h} \le \|u^{(2)} - u_h^{(2)}\|_{\mathcal{F}_h} \cdot \|u^{(2)} - Q_h u^{(2)}\|_{\mathcal{F}_h^+} \\
&+ \|u^{(1)} - u_h^{(1)}\|_{\mathcal{F}_h} \cdot (\|u^{(2)} - Q_h u^{(2)}\|_{\mathcal{F}_h^+} + \|u^{(2)} - u_h^{(2)}\|_{\mathcal{F}_h^+}).
\end{aligned} \tag{5.35}$$

It can be verified directly by (5.35) that

$$\|u^{(2)} - u_h^{(2)}\|_{\mathcal{F}_h} \le C\max\ \{\|u^{(1)} - u_h^{(1)}\|_{\mathcal{F}_h}, \|u^{(2)} - Q_h u^{(2)}\|_{\mathcal{F}_h^+}\}. \tag{5.36}$$

As in the proof of Theorem 4.5 in [16], we can obtain (5.24). ∎

From Lemma 5.1 and 5.2, we obtain the final results as in the proof of Theorem 4.6 in [16].

THEOREM 5.3. *Under the assumptions in Lemma 5.2, we have*

(5.37)

$$\|u - u_h\|_{\mathcal{F}_h} \le C\kappa^{-\frac{1}{2}} h^{s-\frac{3}{2}} \max\{m^{-\lambda(s-1-\varepsilon)+\frac{\delta_\lambda}{2}}, q^{-(s-\frac{3}{2})}\}\left(\|u\|_{s,\kappa,\Omega} + \sum_{l=0}^{s-2}\kappa^{s-l-2}\|f\|_{H^l(\Omega_\delta)}\right),$$

$$\|u - u_h\|_{0,\Omega} \le C(1 + (h\kappa)^{-1})h^{s-1} \max\{m^{-\lambda(s-1-\varepsilon)+\frac{\delta_\lambda}{2}}, q^{-(s-\frac{3}{2})}\}\left(\|u\|_{H^s(\Omega)} + \sum_{l=0}^{s-2}\kappa^{s-l-2}\|f\|_{H^l(\Omega_\delta)}\right).$$

5.2.3. The case of nonhomogeneous Maxwell's equations. Consider nonhomogeneous Maxwell's equations

$$\begin{cases}
\nabla\times\mathbf{E} - i\omega\mu\mathbf{H} = 0 & in \quad \Omega \\
\nabla\times\mathbf{H} + i\omega\varepsilon\mathbf{E} = \mathbf{J} & in \quad \Omega \\
-\mathbf{E}\times\mathbf{n} - \sigma(\mathbf{H}\times\mathbf{n})\times\mathbf{n} = Q(-\mathbf{E}\times\mathbf{n} + \sigma(\mathbf{H}\times\mathbf{n})\times\mathbf{n}) + \mathbf{g} & on \quad \gamma = \partial\Omega,
\end{cases} \tag{5.38}$$

As described in subsubsection 5.1.2, the solution $\mathbf{u} = \begin{pmatrix}\mathbf{E}\\ \mathbf{H}\end{pmatrix}$ of the problem (5.38) is decomposed into $\mathbf{u} = \begin{pmatrix}\mathbf{E} = \mathbf{E}^{(1)} + \mathbf{E}^{(2)}\\ \mathbf{H} = \mathbf{H}^{(1)} + \mathbf{H}^{(2)}\end{pmatrix} = \mathbf{u}^{(1)} + \mathbf{u}^{(2)}$, where $\mathbf{E}^{(1)}$ is the solution of (5.13), and $\mathbf{H}^{(1)}|_{\Omega_k} = \mathbf{H}_k^{(1)} = \frac{1}{i\omega\mu}\nabla\times\mathbf{E}_k^{(1)}$.

It is easy to see that $\mathbf{u}^{(2)} = \begin{pmatrix} \mathbf{E}^{(2)} \\ \mathbf{H}^{(2)} \end{pmatrix} = \begin{pmatrix} \mathbf{E}-\mathbf{E}^{(1)} \\ \mathbf{H}-\mathbf{H}^{(1)} \end{pmatrix}$ is uniquely determined by the following homogeneous Maxwell equations of $\begin{pmatrix} \mathbf{E}^{(2)}\ |_{\Omega_k} \\ \mathbf{H}^{(2)}\ |_{\Omega_k} \end{pmatrix} = \begin{pmatrix} \mathbf{E}_k^{(2)} \\ \mathbf{H}_k^{(2)} \end{pmatrix} = \mathbf{u}_k^{(2)}$:

$$\begin{cases} \nabla\times\mathbf{E}_k^{(2)} - i\omega\mu\mathbf{H}_k^{(2)} = 0 \\ \nabla\times\mathbf{H}_k^{(2)} + i\omega\varepsilon\mathbf{E}_k^{(2)} = 0 \end{cases} \quad in \quad \Omega_k\ (k=1,2,\ldots,N), \tag{5.39}$$

with the following boundary condition on γ and the interface conditions on Γ_{kj} $(k<j;\ k,j=1,\ldots,N)$:

$$\begin{cases} L_k^-(\mathbf{u}_k^{(1)}+\mathbf{u}_k^{(2)}) = -L_j^+(\mathbf{u}_j^{(1)}+\mathbf{u}_j^{(2)}) & on \quad \Gamma_{kj} \\ L_k^-(\mathbf{u}_k^{(1)}+\mathbf{u}_k^{(2)}) = QL_k^+(\mathbf{u}_k^{(1)}+\mathbf{u}_k^{(2)}) + \hat{\mathbf{g}} & on \quad \partial\Omega_k\cap\gamma. \end{cases} \tag{5.40}$$

The variational problem of (5.39)-(5.40) is: to find $\mathbf{u}^{(2)} = \begin{pmatrix} \mathbf{E}^{(2)} \\ \mathbf{H}^{(2)} \end{pmatrix}$ such that

$$\begin{aligned} &\sum_k \int_{\partial\Omega_k} (L_k^+\mathbf{u}_k^{(2)})\cdot\overline{(L_k^+\mathbf{v}_k)}\,ds + \sum_{k\neq j}\int_{\Gamma_{kj}} (L_j^+\mathbf{u}_j^{(2)})\cdot\overline{(L_k^-\mathbf{v}_k)}\,ds \\ &-\sum_k\int_{\gamma_k} Q(L_k^+\mathbf{u}_k^{(2)})\cdot\overline{(L_k^-\mathbf{v}_k)}\,ds \\ &=\sum_k\int_{\gamma_k}\hat{\mathbf{g}}\cdot\overline{(L_k^-\mathbf{v}_k)}\,ds - \sum_{k\neq j}\int_{\Gamma_{kj}}\Big((L_j^+\mathbf{u}_j^{(1)})\cdot\overline{(L_k^-\mathbf{v}_k)} + (L_k^-\mathbf{u}_k^{(1)})\cdot\overline{(L_k^-\mathbf{v}_k)}\Big)ds \\ &+\sum_k\int_{\gamma_k}\Big(Q(L_k^+\mathbf{u}_k^{(1)})\cdot\overline{(L_k^-\mathbf{v}_k)}\,ds - (L_k^-\mathbf{u}_k^{(1)})\cdot\overline{(L_k^-\mathbf{v}_k)}\Big)ds, \quad \forall\mathbf{v}\in\mathbf{V}(\mathcal{T}_h). \end{aligned} \tag{5.41}$$

6. Numerical experiments. In this section we apply the VTCR method and UWVF method to solve several homogeneous and nonhomogeneous Helmholtz and time-harmonic Maxwell equations with complex wavenumbers, and we report some numerical results to compare the accuracy of the approximate solutions generated by the VTCR method, the UWVF method and the PWLS introduced in [16].

For the examples discussed in this section, we adopt a uniform triangulation $\mathcal{T}_h$ for the domain Ω as follows: Ω is divided into small cubes of equal meshwidth, where h is the length of the longest edge of the elements. As described in section 3, we choose the number p of basis functions to be $p=(m+1)^2$ for all elements Ω_k, where m is a variable positive integer.

To measure the accuracy of the numerical solution u_h and $\mathbf{E}_h$, we introduce the relative L^2 error

$$\text{err.} = \frac{||u_{ex}-u_h||_{L^2(\Omega)}}{||u_{ex}||_{L^2(\Omega)}}, \quad \text{or err.} = \frac{||\mathbf{E}_{ex}-\mathbf{E}_h||_{L^2(\Omega)}}{||\mathbf{E}_{ex}||_{L^2(\Omega)}}$$

for analytic solution $u_{ex}\in L^2(\Omega)$, or $\mathbf{E}_{ex}\in(L^2(\Omega))^3$, and

$$\text{err.} = \sqrt{\frac{\sum_j^{Num}|u_{ex,j}-u_{h,j}|^2}{\sum_j^{Num}|u_{ex,j}|^2}}, \quad \text{or err.} = \sqrt{\frac{\sum_j^{Num}|\mathbf{E}_{ex,j}-\mathbf{E}_{h,j}|^2}{\sum_j^{Num}|\mathbf{E}_{ex,j}|^2}}$$

for the exact solution $u_{ex} \notin L^2(\Omega)$, or $\mathbf{E}_{ex} \notin (L^2(\Omega))^3$, where $u_{ex,j}, \mathbf{E}_{ex,j}$ and $u_{h,j}, \mathbf{E}_{h,j}$ are the exact solution and numerical approximation, respectively, of the problem at vertices referred to by the subscript j.

For the examples discussed in this section, we assume that $\mu = 1$. We perform all computations on a Dell Precision T5500 graphics workstation (2*Intel Xeon X5650 and 6*12GECC) using MATLAB implementations.

6.1. A point source smooth problem. The first model problem consists of a point source and associated boundary conditions for homogeneous Helmholtz equation:

$$\begin{aligned} u(\mathbf{r}, \mathbf{r}_0) &= \frac{1}{4\pi}\frac{e^{i\omega|\mathbf{r}-\mathbf{r}_0|}}{|\mathbf{r}-\mathbf{r}_0|} \quad \text{in } \Omega, \\ \frac{\partial u}{\partial \mathbf{n}} + i\kappa u &= g \quad \text{on } \gamma, \end{aligned}$$

in a cubic computational domain $\Omega = [0,1] \times [0,1] \times [0,1]$. $\mathbf{r} = (x, y, z)$ is an observing point. To keep the exact solution smooth in Ω, the location of the source is off-centered at $\mathbf{r}_0 = (2, 2, 2)$ outside the region. In addition, we also consider the singular case in section 6.5.

Tables 1-3 show the L^2 relative errors of the approximations generated by the VTCR method, UWVF method and PWLS method.

TABLE 1
Errors of approximations with respect to p.

	p	9	16	25	36
$\omega = 4\pi - 1i$, $h = \frac{1}{8}$	VTCR	9.27e−2	8.97e−3	1.52e−3	1.08e−4
	UWVF	5.28e−2	5.40e−3	4.99e−4	4.63e−5
	PWLS	2.19e−1	1.83e−2	5.48e−4	4.80e−5
$\omega = 8\pi - 2i$, $h = \frac{1}{16}$	VTCR	1.03e−1	8.49e−3	1.40e−3	9.95e−5
	UWVF	7.54e−2	5.88e−3	4.95e−4	4.81e−5
	PWLS	3.41e−1	3.93e−2	7.12e−4	4.96e−5

TABLE 2
Errors of approximations with respect to h for the case of $\omega = 4\pi - 1i$.

	h	$\frac{1}{4}$	$\frac{1}{8}$	$\frac{1}{16}$
$p = 16$	VTCR	1.43e−1	8.97e−3	6.24e−4
	UWVF	7.75e-2	5.40e−3	3.40e−4
	PWLS	1.72e-1	1.83e−2	1.31e−3
$p = 25$	VTCR	2.71e-2	1.52e−3	1.06e−4
	UWVF	1.41e−2	4.99e−4	1.50e−5
	PWLS	2.09e-2	5.48e−4	2.24e−5

TABLE 3
Errors of approximations with respect to h for the case of $\omega = 8\pi - 2i$.

	h	$\frac{1}{12}$	$\frac{1}{14}$	$\frac{1}{16}$
$p = 16$	VTCR	4.18e−2	1.65e−2	8.49e−3
	UWVF	2.02e-2	1.04e-2	5.88e−3
	PWLS	1.03e-1	6.23e-2	3.93e−2
$p = 25$	VTCR	9.37e−3	4.13e−3	2.10e−3
	UWVF	2.16e−3	9.82e−4	4.95e−4
	PWLS	3.52e-3	1.47e-3	7.12e−4

The results listed in Tables 1-3 indicate that the approximation generated by the UWVF method is much more accurate than that generated by the VTCR method and the PWLS method.

6.2. A nonhomogeneous Helmholtz equation in three dimensions. The exact solution of the second model problem is defined in the closed form

$$u_{\text{ex}} = z\ \ln(1+\omega xy), \quad (x,y,z) \in \Omega,$$

where $\Omega = [0,1] \times [0,1] \times [0,1]$.

We set $\omega = 2\pi$ and choose the number p of the plane wave basis functions as $p = 25$. Table 4 shows the relative L^2 errors of the resulting approximations generated by three methods.

TABLE 4
Errors of approximations with respect to h and q ($\omega = 2\pi,\ p = 25$).

	h	$\frac{1}{4}$	$\frac{1}{5}$	$\frac{1}{6}$	$\frac{1}{7}$	$\frac{1}{8}$
$q = 2$	VTCR	1.01e-1	6.29e-2	4.28e-2	3.09e-2	2.34e-2
	UWVF	1.01e-1	6.29e-2	4.28e-2	3.09e-2	2.34e-2
	PWLS	1.01e-1	6.30e-2	4.28e-2	3.09e-2	2.34e-2
$q = 3$	VTCR	4.74e-2	2.88e-2	1.94e-2	1.40e-2	1.02e-2
	UWVF	4.74e-2	2.88e-2	1.94e-2	1.40e-2	1.02e-2
	PWLS	4.74e-2	2.88e-2	1.95e-2	1.41e-2	1.03e-2

The results listed in Table 4 indicate that the approximations generated by three methods with the local space consisting of third order polynomials is much more accurate than that generated by the corresponding method with the local space consisting of second order polynomials. Moreover, the approximations generated by the VTCR-LSFE method, the UWVF-LSFE method and the PWLS-LSFE method almost have the same accuracy.

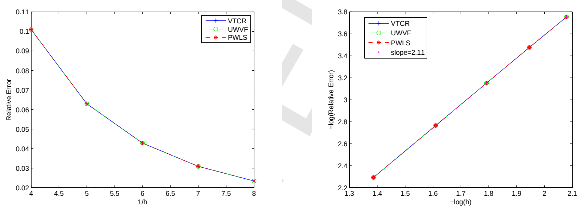

FIG. 1. *(Left): Err. vs* $\frac{1}{h}$. *(Right):* $-log(Err.)$ *vs* $-log(h)$.

Figure 1 (left) and Figure 1 (right) show the plot of Err. with respect to $\frac{1}{h}$ and $-log$(Err.) with respect to $-log(h)$, respectively. It displays a linear plot which verifies the validity of the theoretical results in Theorem 5.3.

6.3. Electric dipole in free space for a smooth case. We compute the electric field due to an electric dipole source at the point $\mathbf{x}_0 = (0.6, 0.6, 0.6)$. The dipole point source can be defined as the solution of a homogeneous Maxwell system (3.17). We set $\mu = 1$ and $\varepsilon = 1 + i$ in (2.12) (σ is determined by μ and ε according to the known formula). The exact solution of the problems is

$$\mathbf{E}_{\text{ex}} = -\mathrm{i}\omega I \phi(\mathbf{x}, \mathbf{x}_0)\mathbf{a} + \frac{I}{\mathbf{i}\omega\varepsilon}\nabla(\nabla\phi \cdot \mathbf{a}) \tag{6.1}$$

where

$$\phi(\mathbf{x},\mathbf{x}_0) = \frac{\exp(\mathrm{i}\omega\sqrt{\varepsilon}|\mathbf{x}-\mathbf{x}_0|)}{4\pi|\mathbf{x}-\mathbf{x}_0|},$$

the amplitude $I = 1$, the vector $\mathbf{a} = (\frac{1.0}{\sqrt{3}}, \frac{1.0}{\sqrt{3}}, \frac{1.0}{\sqrt{3}})$ and $\Omega = [-0.5, 0.5]^3$. To keep the exact solution smooth in Ω, we move the singularity $\mathbf{x}_0$ from $(0.2, 0.2, 0.2)$ (see [17]) in the computational domain to $(0.6, 0.6, 0.6)$ outside the region.

Tables 5-6 show the L^2 relative errors of the approximations generated by the VTCR method, the UWVF method and the PWLS method.

Table 5

Errors of approximations with respect to p.

	p	16	25	36	49	64
$\omega = 2\pi$, $h = \frac{1}{4}$	VTCR	3.52	6.79e−1	1.63e-1	6.60e−1	4.61e-2
	UWVF	3.28e−1	1.67e−1	9.30e−2	4.84e−2	2.55e-2
	PWLS	2.71e−1	1.36e−1	7.48e−2	4.04e−2	2.21e−2
$\omega = 4\pi$, $h = \frac{1}{8}$	VTCR	7.90	2.33	3.74e−1	1.41	9.22e-2
	UWVF	1.72e−1	5.82e−2	1.91e−2	7.06e−3	2.61e−3
	PWLS	1.43e−1	4.56e−2	1.55e−2	5.64e−3	2.01e−3

Table 6

	h	$\frac{1}{4}$	$\frac{1}{8}$	$\frac{1}{12}$
$p = 25, \omega = 2\pi$	VTCR	6.79e−1	2.91e-1	1.72e-1
	UWVF	1.67e−1	3.15e-2	1.14e-2
	PWLS	1.36e−1	2.88e-2	1.11e-2
$p = 36, \omega = 4\pi$	VTCR	9.07e−1	3.74e−1	2.11e−1
	UWVF	1.67e−1	1.91e−2	5.42e−3
	PWLS	1.31e−1	1.55e−2	4.34e−3

The results listed in Tables 5-6 indicate that the approximation generated by the PWLS method is much more accurate than that generated by the VTCR method and possesses slightly higher accuracy than that generated by the UWVF method.

6.4. A nonhomogeneous Maxwell's equations in three dimensions. To illustrate the effectiveness of the proposed approach for nonhomogeneous Maxwell's equations (2.12), we consider the following analytical solution

$$\mathbf{E}_{\mathrm{ex}} = \varepsilon\omega(xz\cos y, -z\sin y, xy)^t, \tag{6.2}$$

where μ and ε are the same as that defined in last subsection. In this example, the source term $\mathbf{J}$ determined by the above solution does not vanish over the entire computational domain $[0, 1]^3$. The discretization of the underlying equations is the same as that of the equations described in Section 5.1.2 and 5.2.3.

We set $\omega = 2\pi$ and choose the number p of the plane wave basis functions as $p = 25$. We report the results of the PWLS-LSFE methd when h decreases and q increases. Table 7 shows the relative L^2 errors of the resulting approximations generated by three methods.

Table 7

Errors of approximations with respect to h and q ($\omega = 2\pi,\ p = 25$).

	h	$\frac{1}{5}$	$\frac{1}{6}$	$\frac{1}{7}$	$\frac{1}{8}$	$\frac{1}{9}$
$q = 2$	VTCR	1.60e-1	1.26e-1	6.72e-2	5.11e-2	4.01e-2
	UWVF	7.91e-2	5.17e-2	3.62e-2	2.65e-2	2.01e-2
	PWLS	1.80e-2	1.21e-2	8.50e-3	6.41e-3	5.00e-3
$q = 3$	VTCR	3.60e-2	2.24e-2	9.80e-3	6.40e-3	4.40e-3
	UWVF	1.78e-2	9.20e-3	5.30e-3	3.30e-3	2.20e-3
	PWLS	4.70e-3	2.32e-3	1.30e-3	7.47e-4	4.58e-4

The results listed in Table 7 indicate that L^2-norm accuracy of the approximation generated by the PWLS-LSFE method is much more accurate than that generated by the UWVF-LSFE method, which possesses slightly higher accuracy than that generated by the VTCR-LSFE method. Moreover, the approximations associated with three order polynomials in local spectral spaces is much more accurate than that associated with two order polynomials in local spectral spaces.

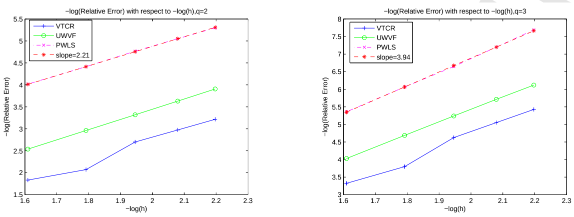

FIG. 2. $-log(Err.)$ vs $-log(h)$.

Figure 2 show the plot of $-log(Err.)$ with respect to $-log(h)$. It displays a linear plot for the PWLS-LSFE and the UWVF-LSFE method.

6.5. A point source singular problem. In this section we compute the acoustic pressure due to a point source at $\mathbf{r}_0 = (0.7, 0.7, 0.7)$. The point source defines the nonhomogeneous Helmholtz equation (5.17) or (5.1). The exact solution of the Helmholtz equation is

$$u(\mathbf{r}, \mathbf{r}_0) = \frac{1}{4\pi} \frac{e^{i\omega|\mathbf{r}-\mathbf{r}_0|}}{|\mathbf{r}-\mathbf{r}_0|} \quad \text{in} \ \ \Omega, \tag{6.3}$$

The Helmholtz equation satisfied by $u(\mathbf{r}, \mathbf{r}_0)$ is an exceptional nonhomogeneous equation whose source term f is just a scalar Dirac function $\delta(\mathbf{r} - \mathbf{r}_0)$. The right-hand side of each subproblem defined by (6.3) is analytically computed in the following way:

$$\int_{\Omega_k} f \, \overline{v_k} \, d\mathbf{r} = \overline{v_k(\mathbf{r}_0)}.$$

The mesh for the case of $\omega = 4\pi - 1i$ consists of 512 elements and 12 800 degrees of freedom (DOFs).

Fig. 3 shows the solutions for the free-space dipole at $\omega = 4\pi - 1i$, where the solutions are computed by (6.3), the PWLS-LSFE method, the UWVF-LSFE method and the VTCR-LSFE method, respectively. The top row shows the real part and the full amplitude of the exact solution, the second row shows the real part of the numerical solutions generated by the three methods, the third row shows the full amplitude of of the numerical solutions. The bottom row presents the distribution of the errors of the approximate solutions generated by the PWLS-LSFE method, the UWVF-LSFE method and the VTCR-LSFE method, respectively.

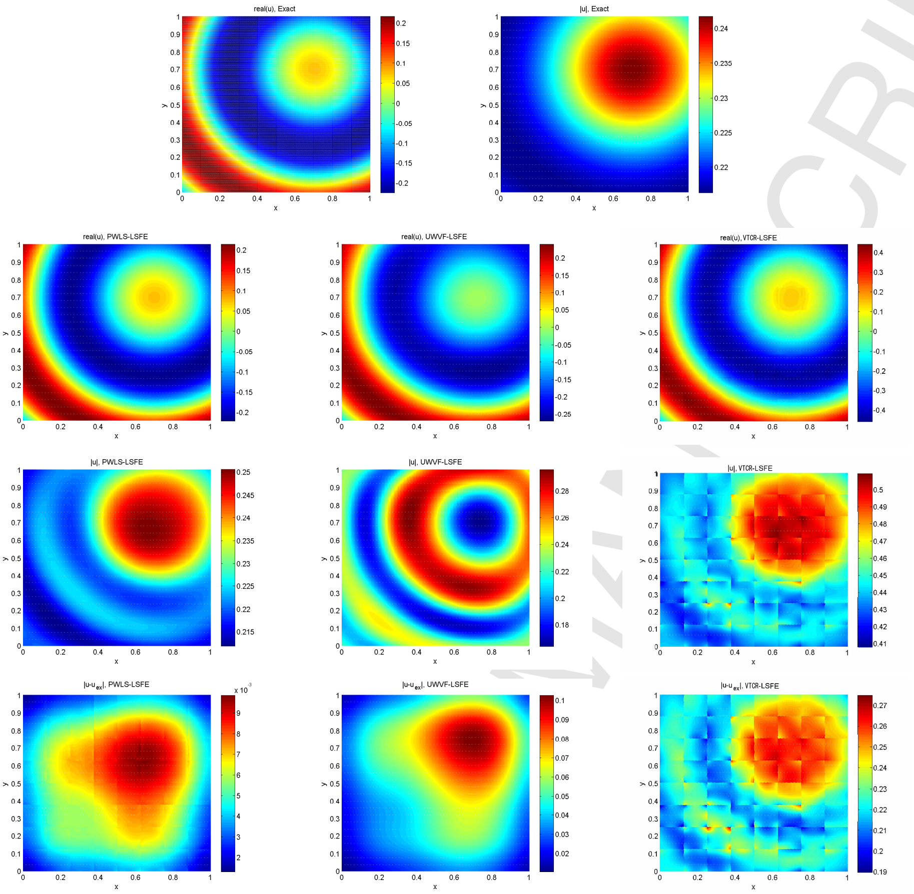

FIG. 3. *Comparision of solutions for the free-space dipole at* $\omega = 4\pi - 1i$ *and* $\lambda/h \approx 4$.

Fig. 3 shows that the approximation generated by the PWLS-LSFE method is much more accurate than that generated by the UWVF-LSFE method, which possesses higher accuracy than that generated by the VTCR-LSFE method.

7. Conclusion. In this paper two variants of the variational theory of complex rays and the ultra weak variational formulation have been introduced for the discretization of the Helmholtz equation and time-harmonic Maxwell equations with complex wave numbers, and have been generalized to discretize the nonhomogeneous Helmholtz equation and Maxwell equatons. The well posedness of the approximate solutions generated by the two methods is derived. The numerical results show that the resulting approximate solution generated by the UWVF method is clearly more accurate than that generated by the VTCR method, and the UWVF method is comparable to the PWLS method in the numerical accuracy.

Acknowledgments. The authors wish to thank the anonymous referees for many insightful comments which led to great improvement in the results and the presentation of the paper.

REFERENCES

[1] M. Amara, R. Djellouli and C. Farhat, Convergence analysis of a discontinuous Galerkin method with plane waves and Lagrange multipliers for the solution of Helmholtz problems, SIAM J. Numer. Anal., 47(2009), pp. 1038-1066.
[2] S. Brenner and L. Scott, Mathematical theory of finite element methods, 3rded., Texts Appl. Math., Springer-Verlag, New York, 2002.
[3] O. Cessenat, Application d'une nouvelle formulation variationnelle aux équations d'ondes harmoniques, Problèmes de Helmholtz 2D et de Maxwell 3D, Ph.d. thesis, Université Paris IX Dauphine, 1996.
[4] O. Cessenat and B. Despres, Application of an ultra weak variational formulation of elliptic PDEs to the two-dimensional helmholtz problem, SIAM J. Numer. Anal., 35(1998), pp. 255-299.
[5] O. Cessenat and B. Despres, Using plane waves as basis functions for solving time harmonic equations with the ultra weak variational formulation, J. Comput. Acous., 11(2003), pp. 227-238.
[6] Y. Du and H. Wu, Preasymptotic error analysis of higher order FEM and CIP-FEM for Helmholtz equation with high wave number. to appear in SIAM J. Numer. Anal.
[7] C. Farhat, R. Tezaur, J. Toivanen. A domain decomposition method for discontinuous Galerkin discretizations of Helmholtz problems with plane waves and Lagrange multipliers. International journal for numerical methods in engineering, 78(2009), No.13, pp.1513-1531.
[8] X. Feng and H. Wu, hp-discontinuous Galerkin methods for the Helmholtz equation with large wave number. Math. Comp., 80(276):1997C2024, 2011.
[9] C. Gittelson, R. Hiptmair and I. Perugia, Plane wave discontinuous Galerkin methods: Analysis of the h-version, ESAIM Math. Model. Numer. Anal., 43(2009), pp. 297-331.
[10] B. Guo. and W. Sun. The optimal convergence of the h-p version of the finite element method with quasi-uniform meshes. SIAM J. Numer. Anal., 45:698C730, 2007.
[11] U. Hetmaniuk, Stability estimates for a class of Helmholtz problems, Commun. Math. Sci., 5(2007), pp. 665-678.
[12] R. Hiptmair, A. Moiola, and I. Perugia, Plane wave discontinuous Galerkin methods for the 2D Helmholtz equation: analysis of the p-version. SIAM J. Numer. Anal., 49(2011), No.1, pp. 264-284.
[13] R. Hiptmair, A. Moiola, and I. Perugia, Error analysis of Trefftz-discontinuous Galerkin methods for the time-harmonic Maxwell equations, Math. Comp., 82(2013), pp. 247-268.
[14] Q. Hu and L. Yuan, A weighted variational formulation based on plane wave basis for discretization of Helmholtz equations, Int. J. Numer. Anal. Model., 11(2014), pp. 587-607.
[15] Q. Hu and L. Yuan, A Plane Wave Least-Squares Method for Time-Harmonic Maxwell's Equations in Absorbing Media, SIAM J. Sci. Comput., 36(2014), pp. A1911-A1936.
[16] Q. Hu and L. Yuan, A Plane wave method combined with local spectral elements for nonhomogeneous Helmholtz equation and time-harmonic Maxwell equations, Adv. Comput. Math., 44(2018), pp. 245-275.
[17] T. Huttunen, M. Malinen, P. Monk, Solving Maxwell's equations using the ultra weak variational formulation, J. Comput. Phys., 223 (2007), pp. 731-758.
[18] T. Huttunen and P. Monk, The use of plane waves to approximate wave propagation in anisotropic media, J. Comp. Math., 25(2007), No. 3, pp. 350-367.
[19] A. Moiola, R. Hiptmair, and I. Perugia, Plane wave approximation of homogeneous Helmholtz solutions, Z. Angew. Math. Phys., 62(2011), pp. 809-837.
[20] P. Monk, Finite element methods for Maxwell's equation, Oxford University Press (2003).
[21] P. Monk and D. Wang, A least-squares method for the helmholtz equation, Comput. Methods Appl. Mech. Engrg., 175(1999), pp. 121-136.
[22] H. Riou, P. Ladevèze, B. Sourcis, The multiscale VTCR approach applied to acoustics problems, J. Comput. Acous., 16(2008), pp. 487-505.
[23] H. Riou, P. Ladevèze, B. Sourcis, B. Faverjon and L. Kovalevsky, An adaptive numerical strategy for the media-frequency analysis of Helmholtz's problem, J. Comput. Acous., 20(2012), https://doi.org/10.1142/S0218396X11004481.
[24] N. Sloane, Tables of spherical codes, http://neilsloane.com/packings/dim3(2014).
[25] R. Tezaur, C. Farhat, Three-dimensional directional discontinuous Galerkin elements with plane waves and Lagrange multipliers for the solution of mid-frequency Helmholtz problems, Int. J. Numer. Meth. Engng., 66(2006), No.5, pp.796-815.
[26] E. Trefftz, Ein gegenstuck zum ritzschen verfahren, Sec. Inte. Cong. Appl. Mech., (1926), pp.131-137.
[27] L. Yuan, The Plane Wave Discontinuous Galerkin Method Combined with Local Spectral Finite Elements for the wave propagation in Anisotropic Media, Numer. Math. Theor. Meth. Appl., 2018, accepted for publication.
[28] L. Yuan and Q. Hu, A solver for Helmholtz system generated by the discretization with wave shape functions, Adv. Appl. Math. Mech., 2013(5), pp. 791-808.
[29] L. Yuan, Q. Hu and Hengbin An, Parallel preconditioners for plane wave Helmholtz and Maxwell systems

with large wave numbers, Int. J. Numer. Anal. Model., 2016,13(5), 802-819.
[30] L. Yuan and Q. Hu, The Plane Wave Methods Combined with Local Spectral Finite Elements for the wave propagation in Anisotropic Media, Adv. Appl. Math. Mech., 2018, accepted for publication.
[31] L. Yuan and Q. Hu, Error analysis of the plane wave discontinuous Galerkin method for Maxwell's equations in anisotropic Media, submitted.